

Impact Craters and Meteorites: The Egyptian Record

L. Folco, W. U. Reimold, and A. El-Barkooky

Contents

11.1 Introduction	416
11.2 Impact Cratering: An Overview	416
11.3 The Impact Record of Egypt	420
11.3.1 Kamil Crater: The Only Confirmed Impact Crater in Egypt.....	420
11.3.2 Proposed and Discarded Impact-Crater Candidates.....	424
11.3.3 Libyan Desert Glass.....	425
11.3.4 Dakhleh Glass.....	432
11.4 Meteorites: An Overview	433
11.5 The Meteorite Record of Egypt	434
11.6 Meteorites in the Archeological Record of Ancient Egypt	437
11.7 Outlook	439
References	441

Abstract

This chapter provides an account of the present Egyptian impact cratering record as well as an overview of the Egyptian meteorite collection. The 45-m-diameter Kamil crater in the East Uweinat District in southwestern Egypt is so far the only confirmed impact crater in Egypt. Due to its exceptional state of preservation Kamil can be considered a type-structure for small-scale impacts on Earth. Enigmatic types of natural glasses including the Libyan Desert glass found in the Great Sand Sea and the Dakhleh glass found

near Dakhla Oasis (note that Dakhla, Dakhleh and Dakhlah are transliterations) may be products of low-altitude airbursts of large and fragile cometary or asteroidal impactors. A number of circular, crater-shaped geological structures superficially resembling impact craters are discussed. To date the Egyptian meteorite collection totals 2 falls, including the ~10 kg Martian meteorite Nakhla that has served as a keystone for the understanding of magmatic differentiation processes on Mars, and 76 finds. With the exception of a minority of incidental findings, most Egyptian meteorite finds (~75%) were recovered over the last ~30 years from three dense meteorite collection areas, namely the El-Shaik Fedl, Great Sand Sea and Marsa Alam fields. The exceptional exposures of the Precambrian basement and Paleozoic to Cenozoic sedimentary covers in Egypt offer a good opportunity for the identification of new impact structures. Likewise, Egypt's vast rocky desert surfaces are of great potential for the collection of meteorites through systematic searches. These prospects are

L. Folco (✉)
 Dipartimento di Scienze della Terra, Università di Pisa,
 Via S. Maria 53, 56126 Pisa, Italy
 e-mail: luigi.folco@unipi.it

W. U. Reimold
 Laboratory of Geochronology, Instituto de Geociências,
 Universidade de Brasília, 70910 900 Brasília, DF, Brazil

A. El-Barkooky
 Department of Geology, Faculty of Sciences, Cairo University,
 Giza, Egypt

fundamental ingredients for fostering the ongoing development of meteoritics and planetary science in Egypt as disciplines for future scientific endeavor in Africa.

11.1 Introduction

The cosmochemical and mineralogical study of meteorites (cm-to-m-sized interplanetary rock debris fallen from space) and the geoscientific study of impact craters produced by the hypervelocity impacts of much larger bodies are of fundamental importance for understanding the geology of the Earth system in a planetary perspective. Impact cratering is one of the most important processes forming and modifying geological surfaces in the solar system. Impact crater structures are—or have been—the main landform on all solid bodies, from asteroids to comets, and from planets to their satellites. Over 50 years of study of the ~200 impact structures recognized to date on the surface of our planet has documented the important role of impacts throughout the history of the Earth, from their local to their global catastrophic effects. Meteorites are rock fragments of a large variety of planetary bodies in the solar system. The great petrologic diversity of meteorites provides a nearly continuous record of planetary evolution, from the early formation of primordial accretional aggregates (chondrites) in the protoplanetary disk to the differentiation of asteroids and terrestrial planets, including the proto-Earth, into metallic cores (iron meteorites) and silicate mantles (achondrites).

In this chapter we provide a detailed account of the present Egyptian impact record and an overview of the Egyptian meteorite collection (Fig. 11.1). Section 11.2 is an overview of the impact cratering process, giving basic information for understanding its importance as a geological process, and for the identification of new impact structures and their ejecta. Section 11.3 first presents the geology of the only impact crater in Egypt confirmed thus far—Kamil Crater (45 m in diameter)—a unique type-structure for investigating the processes and products associated with the impact of small impactors; this is followed by a discussion of the non-impact origin of several crater-like circular structures superficially resembling impact craters in the Western Desert of Egypt, as well as the proposed impact origin of the Libyan Desert Glass and Dakhleh Glass. Section 11.4 is a general introduction to meteorites that highlights their fundamental role in our understanding of the origin and evolution of the solar system. Section 11.5 reports on the 78 meteorites from Egypt to date (September 2018)—including the ~10 kg rare Martian meteorite fall of 1911—Nakhla, their role in the advancement of meteorite

studies, and on the potential of the Egyptian deserts for systematic searches for meteorites. Section 11.6 provides an account of the role of meteoritic iron in the Egyptian archeo-anthropological record and its bearing on the history of human civilization. In the last section 11.7 we discuss a number of perspectives for the future of meteoritics and planetary science in Egypt.

11.2 Impact Cratering: An Overview

Large bolide impact cratering is one of the most important geologic processes in the solar system (e.g., Melosh 1989; Reimold and Jourdan 2012; Hargitai et al. 2015)—and undoubtedly beyond. Impact crater structures are found on the surfaces of all solid bodies in the solar system, from planets to satellites, from asteroids to comets. On many of these bodies, like the Moon or Mercury, impact craters are the dominant landform. On Earth active geodynamics (mainly plate tectonics, erosion and sedimentation) tends to rapidly erase impact structures from the geological record. To date only ~200 impact structures have been confirmed on Earth (<http://www.passc.net/EarthImpactDatabase/>), with the largest and one of the oldest, the 2,020 million year old Vredefort impact structure (South Africa) having originally been ~250–300 km in diameter (Reimold and Koeberl 2014). Evidence of early impact events is rare and recorded only in a small number of impact deposits (so-called spherule layers) with ages of ~2.5 and ~3.5 billion years (Glass and Simonson 2012), many samples of which carry distinctive chemical signatures from the meteoritic impactors. Despite this relatively limited record, interdisciplinary research over the last 50 years has documented the important role of impacts throughout the history of the Earth, from their local to their global catastrophic effects (e.g., Osinski 2008; Reimold and Jourdan 2012; Pierazzo and Artemieva 2012). Catastrophic impact events have had a role in the development of life and have been implicated widely in the debates about the causes of mass extinctions and major evolutionary radiation events. Impact events are indeed destructive, but they may also provide certain economic benefits, including the formation of metalliferous ore deposits, convenient traps for fossil fuel reserves, and locations for water reservoirs (e.g., Reimold et al. 2005). Impact structures can also form new biological niches, which can provide favorable conditions for the survival and evolution of life (Cockell 2006). They can also reveal subsurface stratigraphic information. One of the most outstanding examples is the deeply eroded Vredefort structure, which has provided insight into the nature of the mid-crust and the geological evolution of the Kaapvaal craton over ~3.4



Fig. 11.1 Map of Egypt showing locations of the geological features discussed in this chapter: (i) Kamil crater, the only confirmed impact crater in Egypt (e.g., Folco et al. 2010). (ii) The geological circular features of non-impact origin: El Baz, the Gilf Kebir crater field (GKCF) and Kebira (Reimold and Koeberl 2014). (iii) The strewn field of the Libyan Desert Glass (LDG; green color area). (iv) The collection area of Dakhleh Glass (DG; yellow color area). (v) The find/fall locations of the 78 Egyptian meteorites (orange circles with and without central black dots for falls and finds, respectively) known to date (June 2018) and the boundaries (orange dashed lines) of the three official dense (meteorite) collection areas, as given in the Meteoritical Bulletin database (accessed September 2018, i.e. Great Sand Sea (GSS), Marsa Alam (MA), and El-Shaikh Fedl (ESF). Background image based on Bing and Google Map imagery (see <http://www.google.com>)

billion years (Gibson and Reimold 2008). Finally, many impact structures are sites of great educational value. It is for all these reasons that impact cratering studies have moved into the geological mainstream.

The effective intertwining between geological studies of impact structures on Earth and numerical modeling of the physical processes involved with impacts (Melosh 1989;

Collins et al. 2012) has been instrumental in fostering better understanding of the impact cratering process—a unique, highly dynamic geological process. Extraterrestrial impactors approach Earth at hypervelocity speeds (on average, 18 km/s for asteroids and at least twice this speed for comets). The considerable kinetic energy of such bolides is transferred via a shock front into the target rock, generating

pressures and temperatures that are orders of magnitude greater than those produced by conventional endogenic processes. Rocks are broken, deformed, heated and transformed in unique and irreversible ways. Impact-generated strain rates surpass those of any other geological process by orders of magnitude. Kilometer-scale craters are excavated and collapse gravitationally in minutes, ejecting impact debris on scales that may be continental or global for kilometer-sized impactors. Released gases may cause relatively long-term climate perturbations and elevated temperatures in the crust may persist for thousands of years.

“Impactites” is the collective name for a series of distinct rock types generated by the passage of shock waves (i.e., a compression wave propagating faster than sound) associated with hypervelocity impacts. These impactite types range from purely clastic breccias, composed of fragments of target rock, to impact melt rocks, composed of a groundmass of melt that typically contains clasts of target rock and minerals. A transitional rock type is known as suevite and comprises small bodies of impact melt entrained in a clast-dominated groundmass. Stöffler and Grieve (2007) and Stöffler et al. (2018) have given detailed descriptions of the known impactite types and their recommended nomenclature. The passage of a shock wave first produces compression of the target rock, followed by decompression from peak shock pressures, with concomitant heat generation. Its irreversible effects on rocks and minerals are generally referred to as “shock metamorphism” (or as “impact metamorphism”; e.g. Gillet and El Goresy 2013; Ferrière and Osinsky 2013; Deutsch et al. 2015; Stöffler et al. 2018).

On the Moon and other solid planetary bodies in the solar system that are characterized by the lack of an atmosphere and of plate tectonics, impact craters are well preserved features, and can be recognized from their characteristic morphologies and structures. These vary progressively with increasing energy of the impact from relatively small simple bowl-shaped craters to relatively large (up to hundreds or thousands of km in diameter) complex crater structures, including the morphologies of central peak craters, peak-ring craters, and multi-ring basins (e.g., Reimold and Koeberl 2014; Hargitai et al., 2016).

On Earth identification of impact structures is often difficult, mainly due to the destructive effects of weathering, erosion, tectonic deformation, or burial of impact craters and possible remnants of the impactors. Fresh impact structures typically are characterized by a raised rim with overturned stratigraphy; extensive fracturing and brecciation are

additional characteristic features but those alone are not diagnostic. In the interest of improving Earth’s impact cratering record, diagnostic criteria for accurate identification and confirmation of impact structures and their deposits on Earth have been developed to overcome these problems (e.g., French and Koeberl 2010; Reimold and Koeberl 2014). Diagnostic evidence for impact events may be present in the target rocks that were affected by the impact—either in exposed target rock of the crater floor or, when present, a central stratigraphically uplifted terrain known as “central uplift”—and in breccia occurrences that may be found within a suspicious structure or perhaps outside. Circular structures that are anomalous in the regional geologic context, or circular or annular geophysical anomalies are possible indicators of impact crater structures. However, neither is diagnostic and an impact origin must be confirmed by the presence of any of the following key features (Fig. 11.2):

- i. Shatter cones: a conical-to-subconical fracture phenomenon in rock, with narrow striae emanating from a small apex area. The formation process of shatter cones is still debated (Baratoux and Reimold 2016). However, this distinctive fracturing phenomenon to date has only been described from impact structures (and nuclear explosion sites), where they are formed in the shock pressure range from ~ 2 to 30 GPa. They occur at scales from centimeters to meters and are the only known meso- to macroscopic impact-diagnostic criterion.
- ii. Diagnostic shock-metamorphic effects, including planar deformation features, deformation twins in zircon; diaplectic glass after silicate minerals; high-pressure mineral polymorphs such as diamond (after graphite), coesite and stishovite (after quartz), reidite (after zircon)—all mineral polymorphs that are not formed by other geological processes in rocks of the upper crust, or ringwoodite or wadsleyite (after olivine)—and many other high-pressure minerals discovered in meteorites (e.g., Langenhorst and Deutsch 2012; Ferrière and Osinsky 2013; Deutsch et al. 2015; Cavosie et al. 2018).
- iii. It may also be possible to identify, admittedly rarely, remnants of the extraterrestrial impactors in the form of fragments of a meteorite, or traces of projectiles in impact breccias through detection of their chemical or isotopic extraterrestrial signatures (e.g., Koeberl et al. 2012; Goderis et al. 2013; Koeberl 2014).

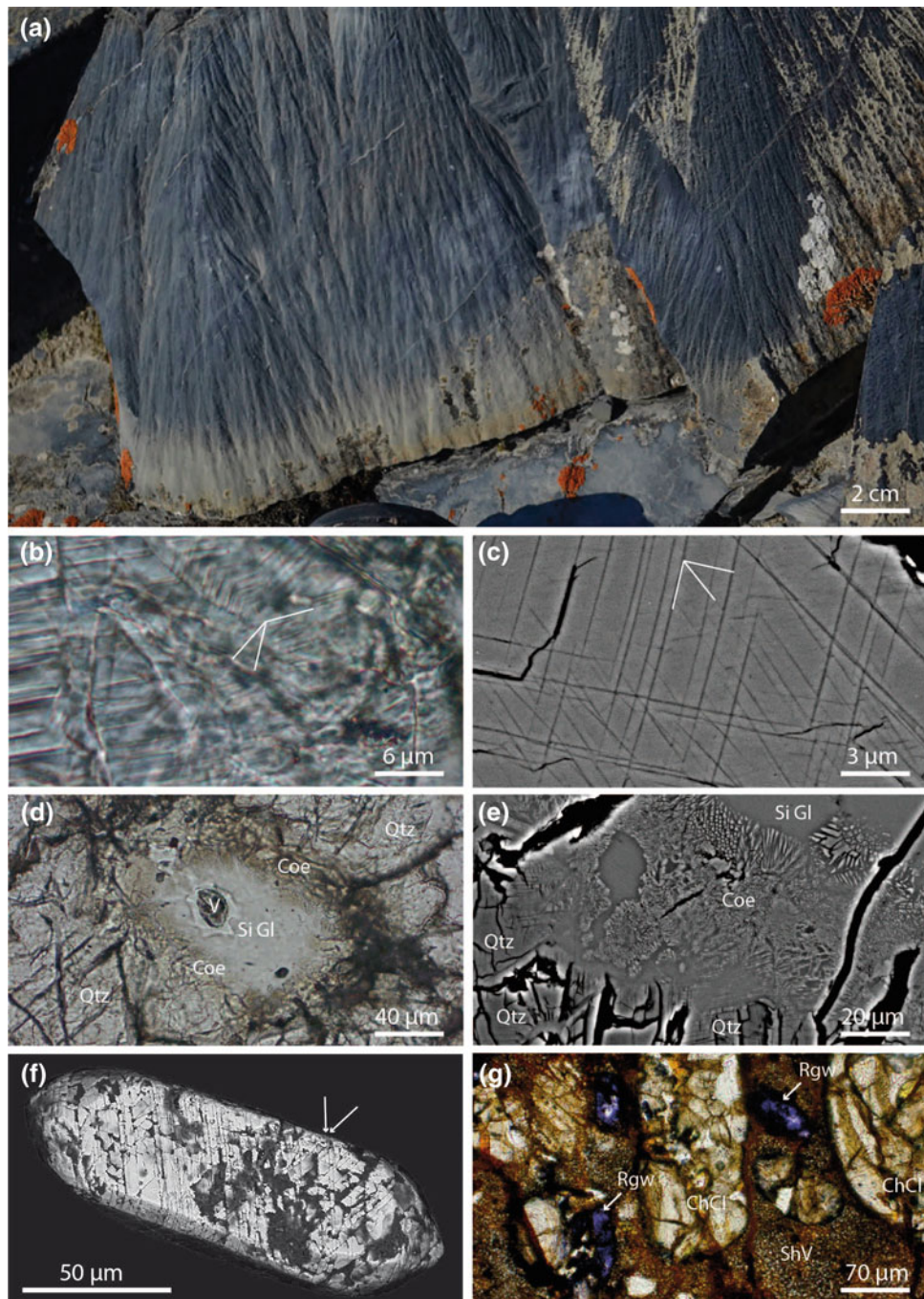


Fig. 11.2 A selection of key shock metamorphic features. **a** Shatter cones in fine-grained Neoproterozoic limestone in an outcrop at the center of the ~25-km-diameter Tunnunik crater (Canada). Image courtesy of Pierre Rochette (CEREGE, France). **b** Optical micrograph of planar deformation features (PDF) in a quartz crystal from a shocked sandstone found in the ejecta deposit around the 45-m-diameter Kamil Crater (Egypt, Fig. 11.1). The orientations of three sets of PDF are indicated. **c** Back-scattered electron image of PDF (three sets are indicated) in a quartz crystal from the same rock. Image courtesy of Agnese Fazio (Friedrich-Schiller—Universität Jena). **d** Optical micrograph showing an intergranular assemblage of microcrystalline coesite (brown) set in silica glass in a shocked sandstone from Kamil Crater. **e** Back-scattered electron image of the same feature. **f** Back-scattered electron image of a detrital shocked zircon found in the Vaal River of South Africa (after Erickson et al. 2013). The zircon grain was eroded from shocked bedrock of the ~2.0 Gyr-old Vredefort impact structure. Planar microstructures visible on the surface of the grain (see arrows) are a manifestation of shock damage of zircon. These features were shown to be {112} deformation twins which form in zircon at ~20 GPa, conditions only created in Earth's crust during meteorite impacts. Image courtesy of Aaron Cavosie, Curtin University, Western Australia. **g** Optical micrograph of ringwoodite crystals (purple) set in a dark, clast laden, microcrystalline shock vein of a highly shocked chondritic (DaG 528) meteorite. Image courtesy of Fabrizio Campanale (Università di Pisa, Italy). Abbreviations: Coe = coesite; Qtz = quartz; SiGl = Silica glass; V = vesicle; Rgw = ringwoodite; ChCl = chondritic clast; ShV = shock vein

11.3 The Impact Record of Egypt

11.3.1 Kamil Crater: The Only Confirmed Impact Crater in Egypt

Kamil Crater in the East Uweinat District, southwestern Egypt (22°01'06" N, 26°05'15" E Fig. 11.1), is a 45-m-diameter impact crater with a pristine ejecta ray structure in its environs (Fig. 11.3; Folco et al. 2010). Formed less than 5,000 years ago by the hypervelocity impact of an iron meteorite named Gebel Kamil, it is the only confirmed impact structure in Egypt so far. The structure was identified in 2008 by V. De Michele (former curator of the Natural History Museum in Milan, Italy) during a Google Earth™ survey. Two years later, field work carried out as part of the 2010 Italian-Egyptian geophysical investigation confirmed the impact origin of the structure (Folco et al. 2010).

Folco et al. (2011) and Urbini et al. (2012) reported that the crater occurs on exposed pale sandstones (mainly quartz arenites) of the Gifl Kebir Formation (Early Cretaceous) that are locally overlain by a few centimeters of loose soil. The sandstones have subhorizontal bedding and constitute part of the sedimentary cover unconformably overlying the Precambrian crystalline basement. The crater has all the characteristic features of simple craters including a bowl shape and a raised rim (raised up to ~3 m above the presumed pre-impact surface). The true crater floor, at an average depth of 16 m below rim crest, is overlain by an ~6-m-thick crater-fill consisting of displaced blocks and stratified fallout debris. At crater walls, bedding of the bedrock is upturned (up to 40°) and dips radially outward. An overturned flap of ejected material is locally present at the rim crest. The bulk of the debris ejected from the impact crater consists of sandstone fragments ranging from large boulders, with masses up to 4 tons, to dust. Their pale color sharply contrasts with the darker color of the weathered bedrock (Fig. 11.3). A continuous ejecta blanket extends radially for ~50 m from the crater rim in a northward, eastward, and southward direction. Three ejecta rays extend for as much as 350 m from the crater rim and trend to the north, southeast, and southwest. Such well-preserved structures have been previously observed only on airless extraterrestrial rocky or icy planetary bodies and attest to the exceptional freshness of the structure.

Through systematic visual searches, over 5000 iron meteorite specimens amounting to a total of 1.7 tons were identified within the crater and in its vicinity (Fig. 11.4; Folco et al. 2010, 2011; D'Orazio et al. 2011). They all have the characteristics of shrapnel produced by fragmentation of the impactor upon impact with masses ranging up to ~34 kg (Fig. 11.4a, b), except for one regmaglypted, partly

fusion-crust individual of ~90 kg mass (Fig. 11.4c) that likely detached from the main impact body during atmospheric flight. This led Folco et al. (2010, 2011) to suggest that Kamil Crater was generated by an impactor that hit the ground nearly intact without significant fragmentation in the atmosphere. Meteoritic debris (shrapnel) is concentrated in terms of mass and number towards the southeast of the crater, whereas it is virtually absent in the northwestern quadrant (Fig. 11.4d). This asymmetric distribution defines the downrange jet of impactor debris produced by an oblique impact from the northwestern quadrant. Putting together the total mass of meteorite specimens found during systematic visual searches (D'Orazio et al. 2011), of specimens buried in the ejecta that could be detected through a magnetic survey (Urbini et al. 2012), and of microscopic impactor debris found in the soil around the crater, the projectile mass was estimated at about 10 tons (Folco et al. 2015). Noble gas and radionuclide analyses of the Gebel Kamil iron meteorite by Ott et al. (2014) point to a pre-atmospheric mass > 20 tons, but it may have been as much as 50–60 tons.

D'Orazio et al. (2011) provided a detailed account of the petrography and geochemistry of the Gebel Kamil meteorite. The meteorite is classified as an ungrouped Ni-rich ataxite (Ni = 19.8 weight% [wt%], Co = 0.75 wt%, Ga = 49.5 $\mu\text{g g}^{-1}$, Ge = 121 $\mu\text{g g}^{-1}$, Ir = 0.39 $\mu\text{g g}^{-1}$).

Fazio et al. (2014, 2016) carried out petrographic studies of samples from the crater wall and from ejecta deposits collected during the 2010 geophysical campaign in order to investigate shock effects recorded by small impact craters on Earth. They reported a wide range of shock metamorphic features indicative of a range of high pressures (locally up to ~60 GPa) and temperatures (even in excess of ~1700 °C) typical of hypervelocity impacts. These features include:

- (i) Ill-developed shatter cones, pseudotachylitic breccia veinlets in sandstone specimens found in the ejecta, planar deformation features in quartz (Fig. 11.2b, c), the high-pressure silica polymorphs coesite (Fig. 11.2d, f) and stishovite, lechatelierite (silica glass), baddeleyite as decomposition product after zircon in shocked target sandstone.
- (ii) Impact melt lapilli, bombs and microscopic impact spherules found scattered around the crater (Fig. 11.5). The impact velocity was estimated to have been at least some 3.5 km s⁻¹. Later, Fazio et al. (2016) and Hamann et al. (2018) conducted a detailed petrographic and geochemical investigation of impact melt glasses to improve our understanding of the projectile-target interaction during impact melting.

Based on geo-archeological reasoning, namely the chronological relationship between the impact structure and

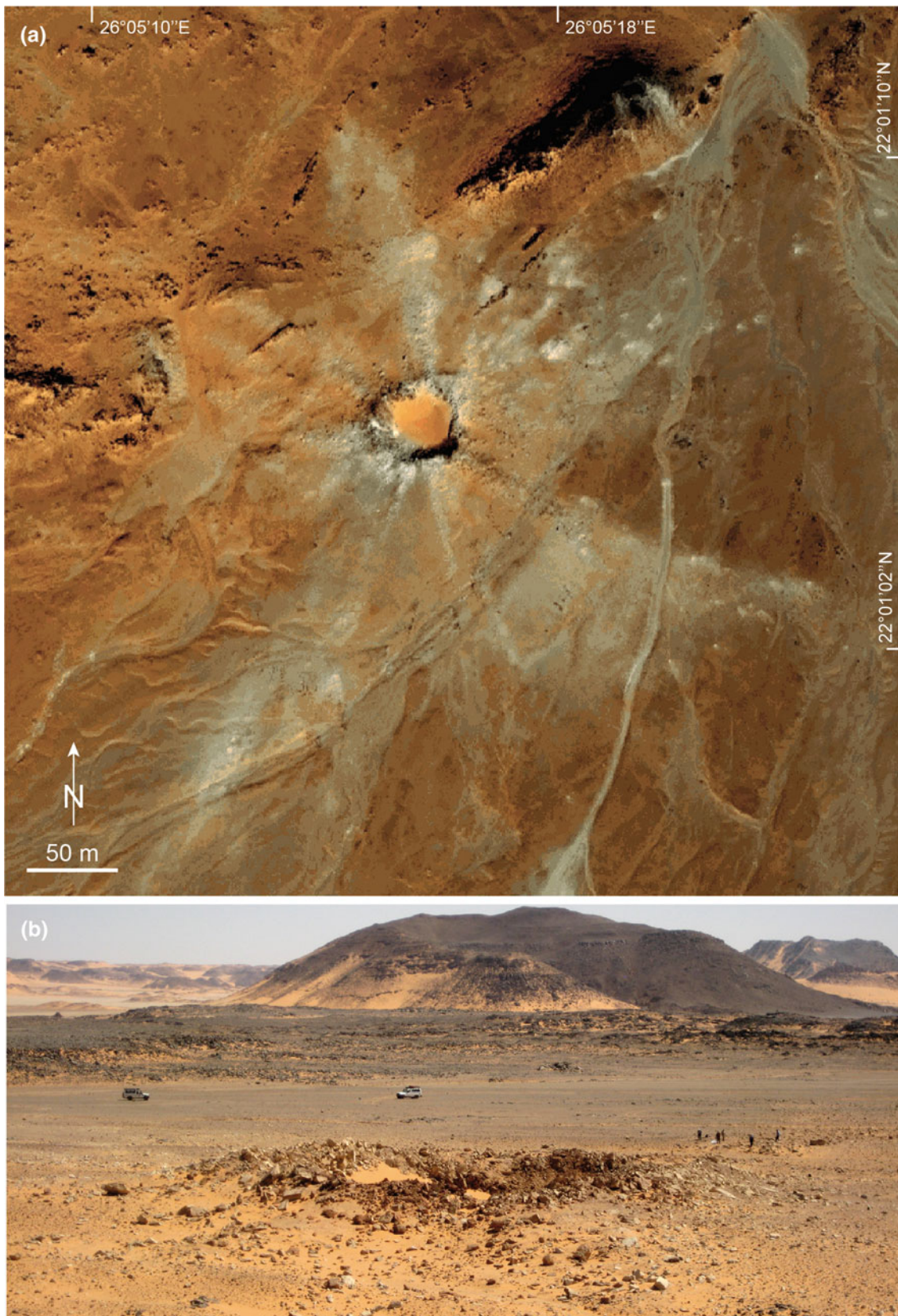


Fig. 11.3 The 45-m-diameter Kamil Crater, southwestern Egypt (22°01'06" N, 26°05'15" E; location map in Fig. 11.1) (after Folco et al. 2010, 2011). QuickBird satellite image (22 October 2005; courtesy of Telespazio); note simple crater structure and prominent ejecta ray pattern indicative of an exceptional state of preservation. Inset: Location map. B) View of the crater from the west

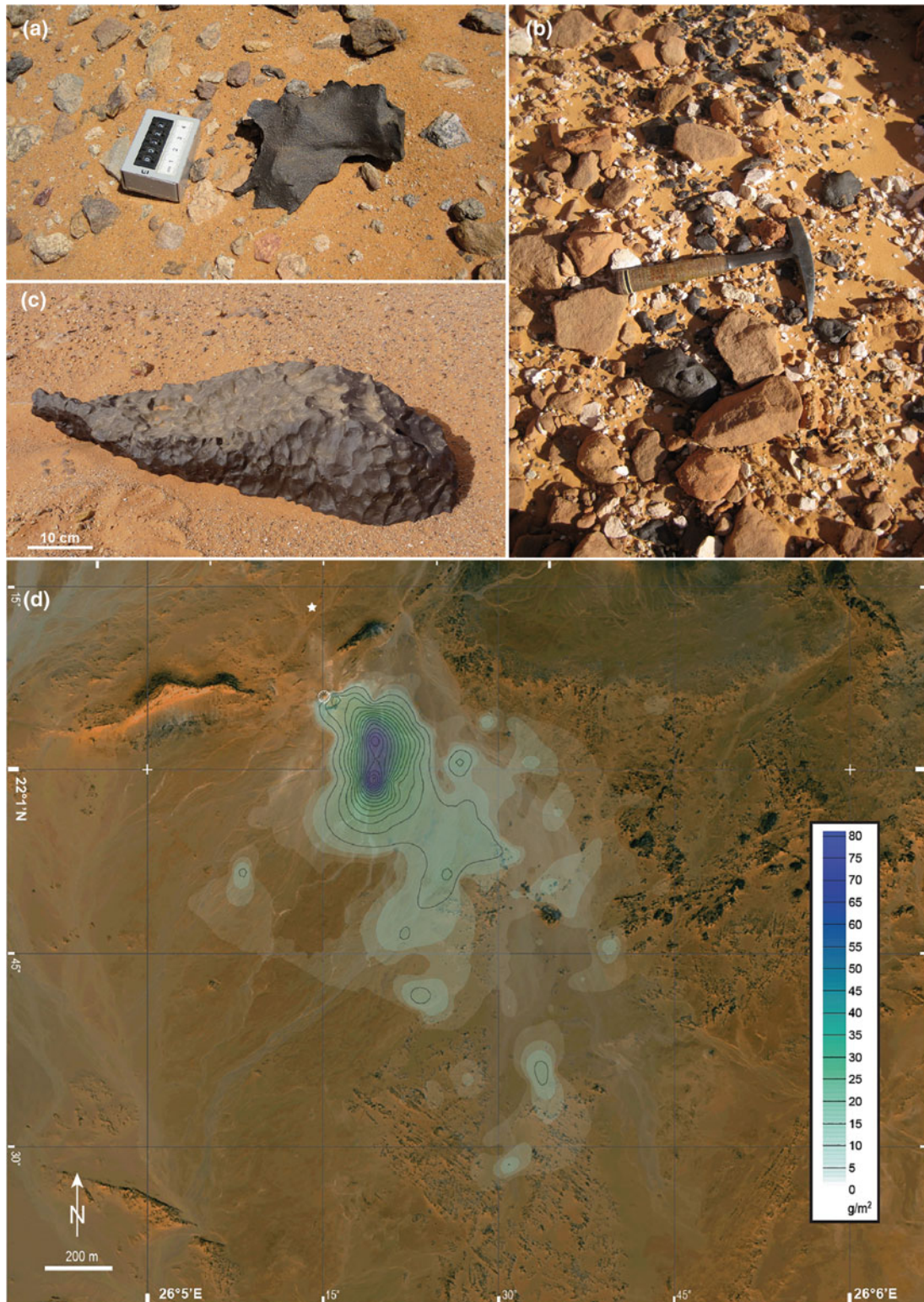


Fig. 11.4 The iron meteorite named Gebel Kamil (after Folco et al. 2011; D’Orazio et al. 2011). **a** Field photograph of one of the thousands of meteorite fragments (shrapnel) found scattered in the crater and surrounding area. **b** Local concentration of tens of iron meteorite shrapnel occurring close to the southeast rim of the crater. **c** Field photograph of the ~ 83 kg meteorite specimen with regmaglypts found ~ 230 m due north of the crater. **d** Gebel Kamil meteorite distribution map (g/m^2) obtained through linear interpolation of average meteorite density values for $50 \text{ m} \times 50 \text{ m}$ cells, with values positioned at their centers. Contour lines are shown at $5 \text{ g}/\text{m}^2$ intervals. The white star shows the original location of the 83 kg individual (D’Orazio et al. 2011). Image courtesy of Massimo D’Orazio (Universita di Pisa, Italy)

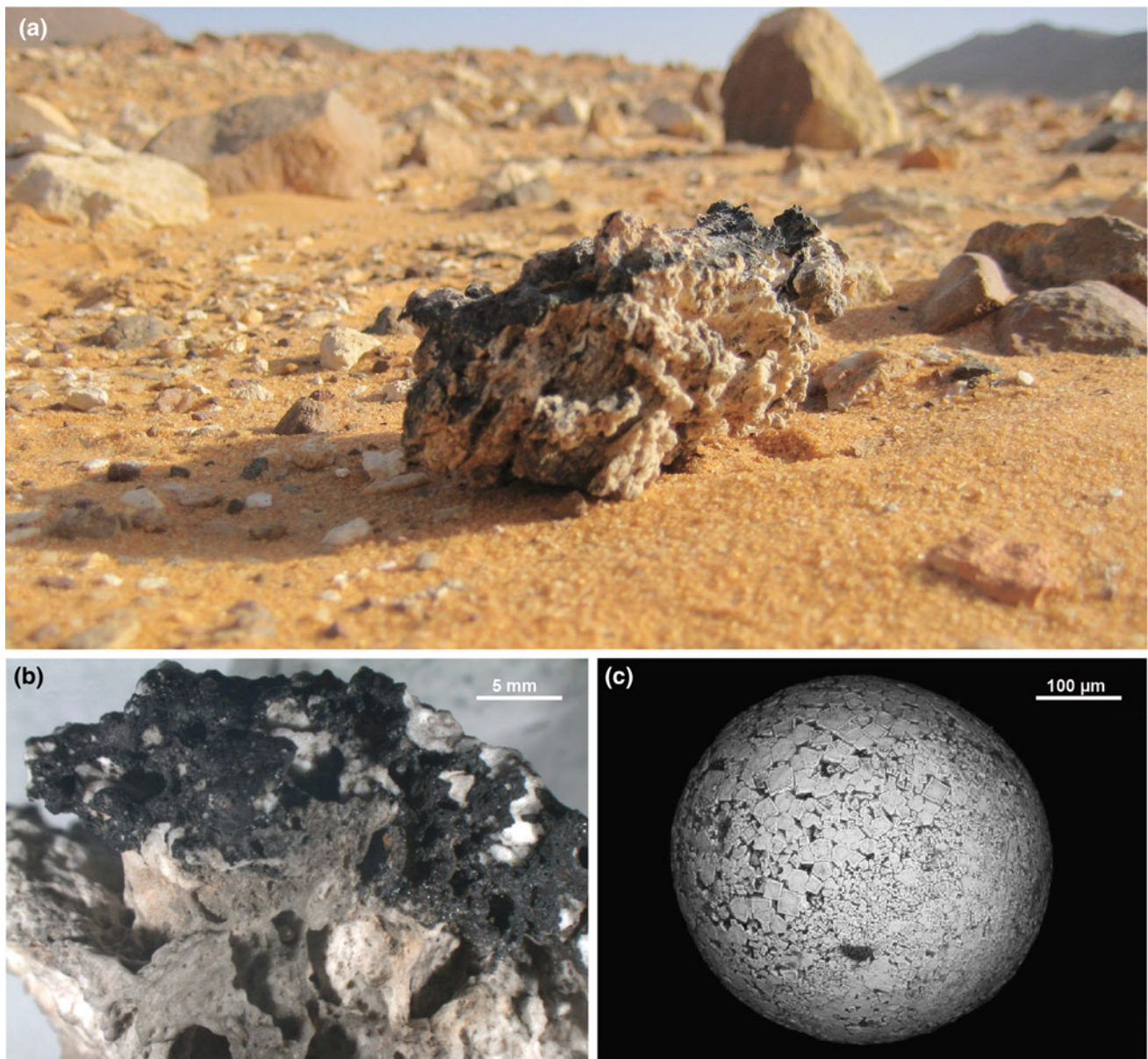


Fig. 11.5 Impact melt glass and spherules from Kamil Crater. **a** A fist-sized pumiceous impact glass specimen found scattered in the ejecta blanket. The white part of the specimen consists of silica-rich glass derived from the melting of the target sandstone. The darker parts are enriched in Fe and Ni as a result of mixing with projectile melt. **b** A section of the same specimen showing increasing darker colors with increasing projectile versus target components. **c** Back-scattered electron image of a microscopic impact melt spherule consisting mainly of Fe-Ni oxides and traces of interstitial silica-rich glass

a number of features (trails, settlements) attesting to pre-historic human occupation of the area, Folco et al. (2011) suggested that the impact event occurred less than 5000 years ago. This young age was later confirmed by thermoluminescence dating of quartz in the shocked target rocks, which yielded a formation age constrained between 2000 BCE and 500 CE, with a favored age interval between 1600 and 400 BCE (Sighinolfi et al. 2015).

Small impact craters (<300 m in diameter) are rare on Earth, and those known are mostly deeply eroded. A number of features attest to the extraordinary state of preservation of Kamil Crater: the bright ejecta rays, the large inventory of shock metamorphic features, and the remnants of fusion crust on a specimen of the iron projectile. Kamil can be considered a type-structure for small-impact craters on Earth and as such, as a natural laboratory to investigate the

processes and products associated with the impact of small projectiles (Folco et al. 2011).

11.3.2 Proposed and Discarded Impact-Crater Candidates

A number of crater-shaped geological structures in Egyptian territory, mainly identified remotely through satellite image analysis, were eventually proven to be of non-impact origin, mainly based on subsequent field work. They are the thousands of circular to elliptical structures in the Gilf Kebir region known in the literature as El Baz (El-Baz 1981), the Gilf Kebir Crater Field (e.g., Paillou et al. 2004) and Kebira (El-Baz and Ghoneim 2007).

11.3.2.1 El-Baz

Through Landsat satellite image analysis, El-Baz (1981) identified a circular structure ~ 4 km in diameter, located at $24^{\circ}12' N$, $26^{\circ}24' E$ (Figs. 11.1 and 11.6), among the linear dunes of the Great Sand Sea of Egypt. The structure, denominated El-Baz Crater, occurs in sandstones of the Nubia Formation (note that this is a term traditionally used in a broad range of stratigraphical and sedimentological connotations to designate a thick series of quartzose sandstones overlying the igneous and metamorphic Archean to Lower Paleozoic basement rocks). The structure is characterized by a flat floor, terraced walls, crenulated rim, and subdued remains of a central feature ~ 1.6 km in diameter. The alleged crater is surrounded by a rough-textured deposit containing large boulders and extending up to 2 km from the crater rim. El-Baz (1981) interpreted the structure as an impact crater based on its overall morphology, similar to that of the bowl-shaped Barringer Crater (aka Meteor Crater) in Arizona, USA. He also noted, however, that the structure could also have been formed by a circular diorite intrusion. The site was visited in 2005 by an Italian geological expedition: Orti et al. (2008) concluded that the El-Baz Crater was one of the many volcanic circular features in the region that are defined by basaltic dikes intruded into the quartz-arenitic bedrock.

11.3.2.2 The Gilf Kebir Crater Field

In 2004, Paillou et al. identified numerous roughly elliptical to circular structures up to several kilometers in diameter through space-borne radar imaging analysis in an area of 4500 km^2 due east of the Gilf Kebir plateau (Figs. 11.1 and 11.7). Field work conducted on 13 structures from 20 m to 1 km in diameter led the research team to propose that they had discovered the largest impact crater field on Earth, possibly created by several meteorites that broke up when entering the atmosphere. Shock deformation in the form of

planar deformation features in breccias and shatter cone-like features were alleged as positive evidence for an impact origin of these structures.

Two years later, Paillou et al. (2006) reported the results of an extended satellite imagery analysis of the Gilf Kebir region. Over an area of $40,000 \text{ km}^2$, more than 1300 circular crater-like structures with a typical size of 150 m had been identified. The size and number of the structures, coupled with geological data obtained from field work on a selection of 62 structures, led the team to discuss the alternative hypothesis of a hydrothermal vent complex for the origin of these structures.

In 2005, an Italian expedition (Orti et al. 2008) visited this region and carried out structural geological analysis and geophysical surveys, followed by petrographic and geochemical investigations on samples. They also presented a detailed geological account of the geology of the region surrounding the Gilf Kebir plateau. Extending for $\sim 8000 \text{ km}^2$, the Gilf Kebir Plateau is ~ 1100 m high and ~ 300 m above the desert floor. It comprises Paleozoic-Mesozoic clastic Cretaceous to Lower Tertiary sedimentary units of the “Nubia Sandstone”, locally covered by Quaternary sand dunes and sheets (Issawi 1982; Klitzsch et al. 1987).

Orti et al. (2008) found that of the 62 structures previously investigated by Paillou et al. (2006) ten structures could be directly associated with basalt dikes. Geophysical data acquired at selected structures did not show the bowl-shaped geometries characteristic of small impact craters. Oblique sandstone layers at the rims of some crater structures dip toward the center of the crater, in contrast to what is expected at small impact craters where uplifted bedding at the crater walls radially dips outwards. Breccias with no characteristic shock deformation features were interpreted as intraformational sedimentary breccias or tectonic breccias. Striations on sandstone and basaltic rocks previously interpreted as shatter cones were recognized as wind-abrasion features.

Orti et al. (2008), thus, determined that the earlier observations were inconsistent with an impact origin for these crater-like structures in the Gilf Kebir area. They concluded that these features are likely related to endogenic processes typical of hydrothermal vent complexes in volcanic areas, which may reflect the emplacement of subvolcanic rocks.

11.3.2.3 Kebira

The name Kebira is an Arabic word, which means “large”. It is a circular topographic feature identified by El-Baz and Ghoneim (2007) using satellite imagery, Radarsat-1, and Shuttle Radar Topography Mission (SRTM) data. This feature lies to the west of the Gilf Kebir Plateau straddling the border between Egypt and Libya ($\sim 24^{\circ}39' N$, $24^{\circ}58' E$; Figs. 11.1 and 11.8). Based solely on the remote sensing data, El-Baz and

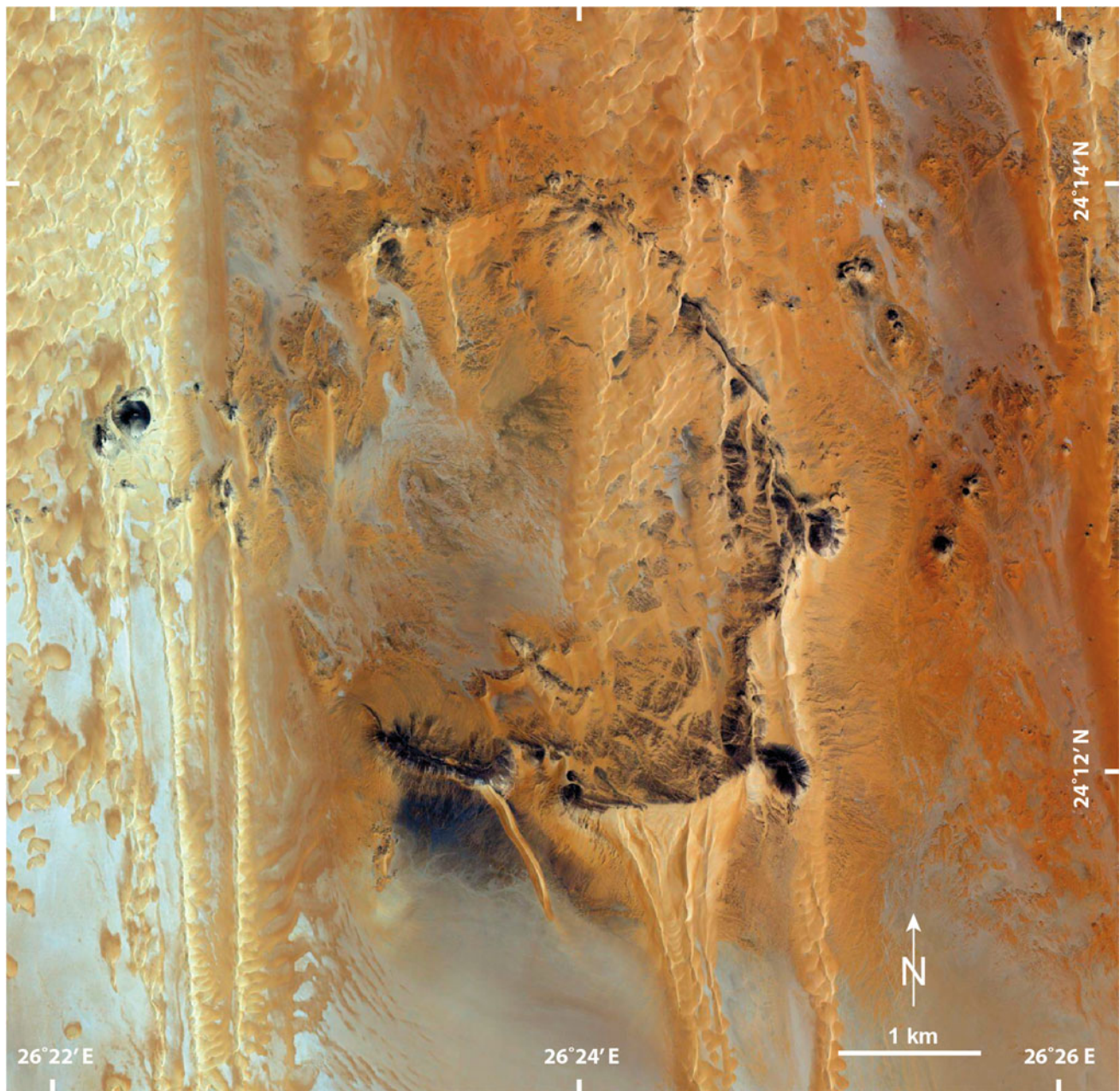


Fig. 11.6 The El-Baz circular (~ 4 km in diameter), crater-like feature listed amongst the discredited impact proposals (location map in Fig. 11.1). The feature is delimited by basaltic dikes intruded into the quartz-arenitic bedrock and is of volcanic origin (Orti et al. 2008)

Ghoneim (2007) argued that this feature is an exceptionally large (31 km in diameter), double-ringed, impact crater. They suggested that the crater's original morphology had been obscured by wind and water erosion over time. They neither conducted any fieldwork at this feature nor studied any samples collected from it. The alleged "central uplift" retains the horizontal bedding of the surrounding sandstone plateau without indication of stratigraphic uplift, providing clear evidence against a possible impact origin.

11.3.3 Libyan Desert Glass

Libyan Desert Glass (LDG) is an enigmatic, high-silica, natural glass found along the southwestern margin of the Great Sand Sea (Fig. 11.1). The origin of this glass has been a matter of debate since its first scientific investigation in 1932 (Clayton and Spencer 1933). Hundreds of scientific papers have been published about the physical-chemical properties of the LDG, and the vast majority of these agree

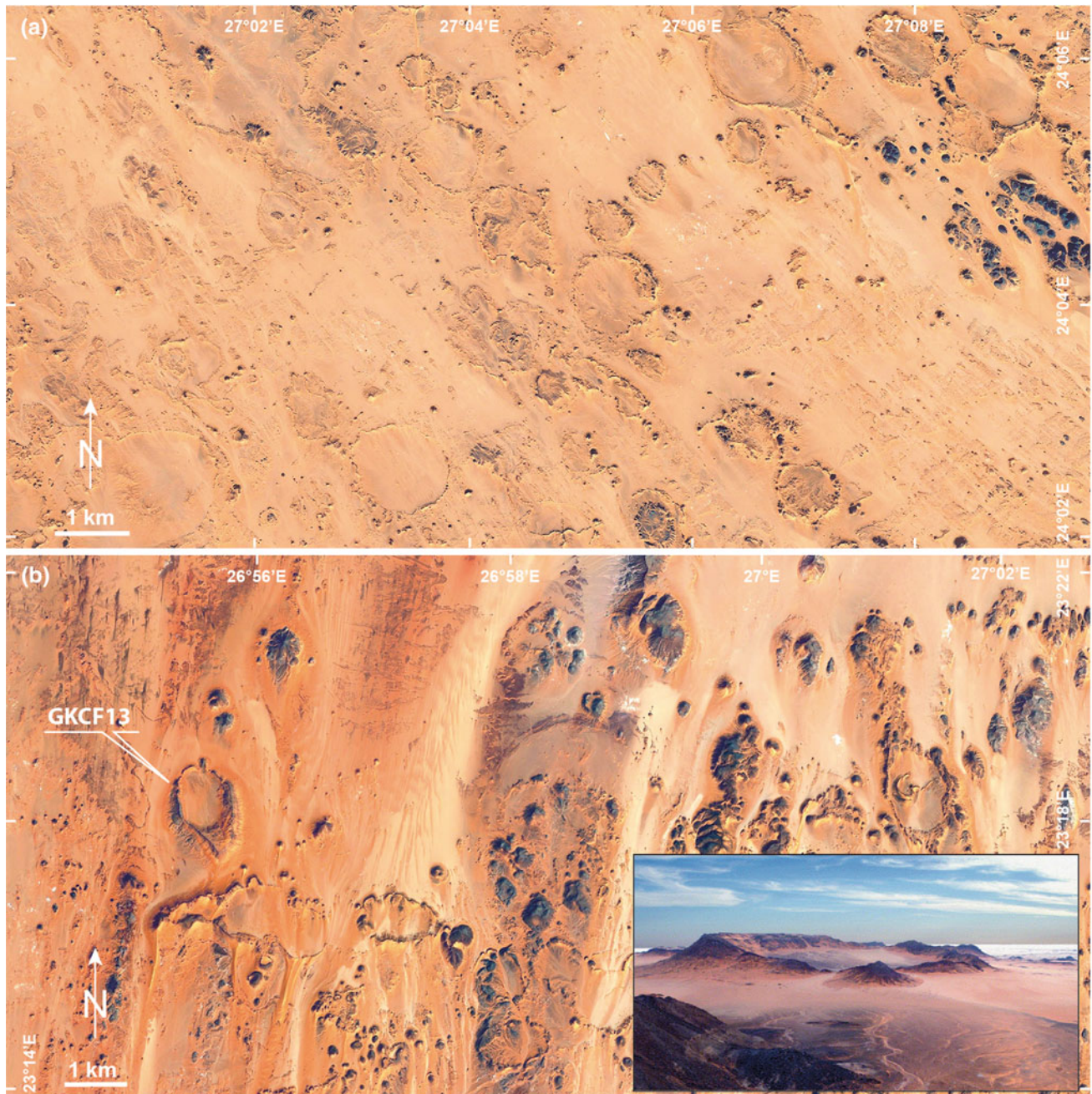


Fig. 11.7 Google Earth images of crater shaped geological features of non-impact origin in the Gifl Kebir region (location map in Fig. 11.1. **a** A portion of the study site 2a investigated by Paillou et al. (2006). **b** A portion of the study site “3a” investigated by Paillou et al. (2006). The inset shows a view from the north-northeast of the ~950-m-diameter crater-like structure denominated GKCF13 by Paillou et al. (2006). All these circular features are seemingly of volcanic origin (Orti et al. 2008)

that it is an impact glass; yet no source crater has been identified so far.

LDG occurs in the form of irregularly-shaped masses up to a few tens of cm in size (Fig. 11.9) that are found strewn across the exposed surface of sandstone bedrock (Cretaceous Nubia Formation) in the linear corridors between

the ~100 m high and 3–5 km apart, ~N-S—trending seif sand dunes of the Great Sand Sea. The glass is found discontinuously over a nearly oval area of $\sim 95 \times 30 \text{ km}^2$ (Weeks et al. 1984), with a major concentration around $\sim 25^\circ 25' \text{ N}$, $25^\circ 30' \text{ E}$ (Barakat et al. 1997). Existing estimates of the amount of glass present on the surface are in

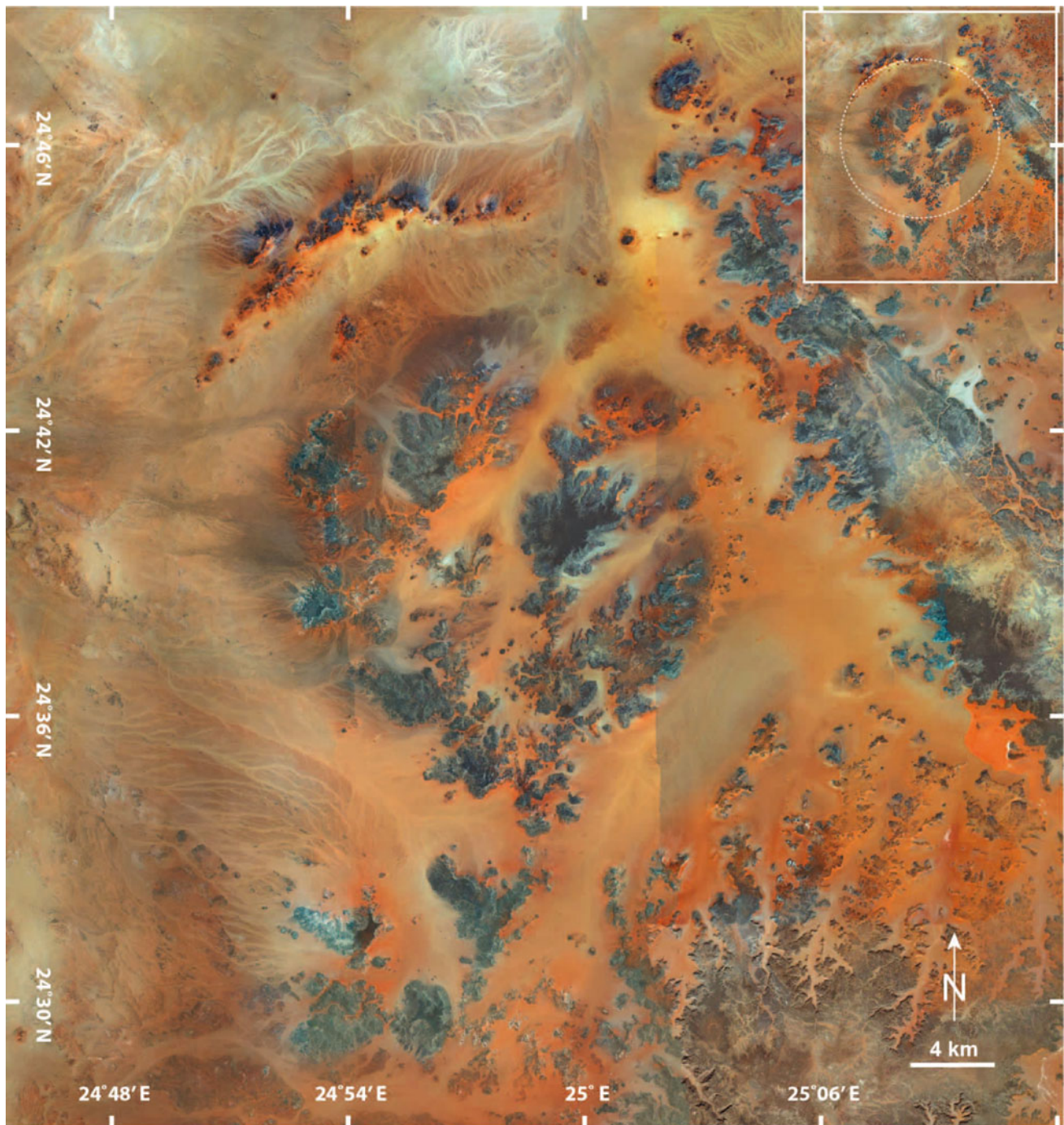


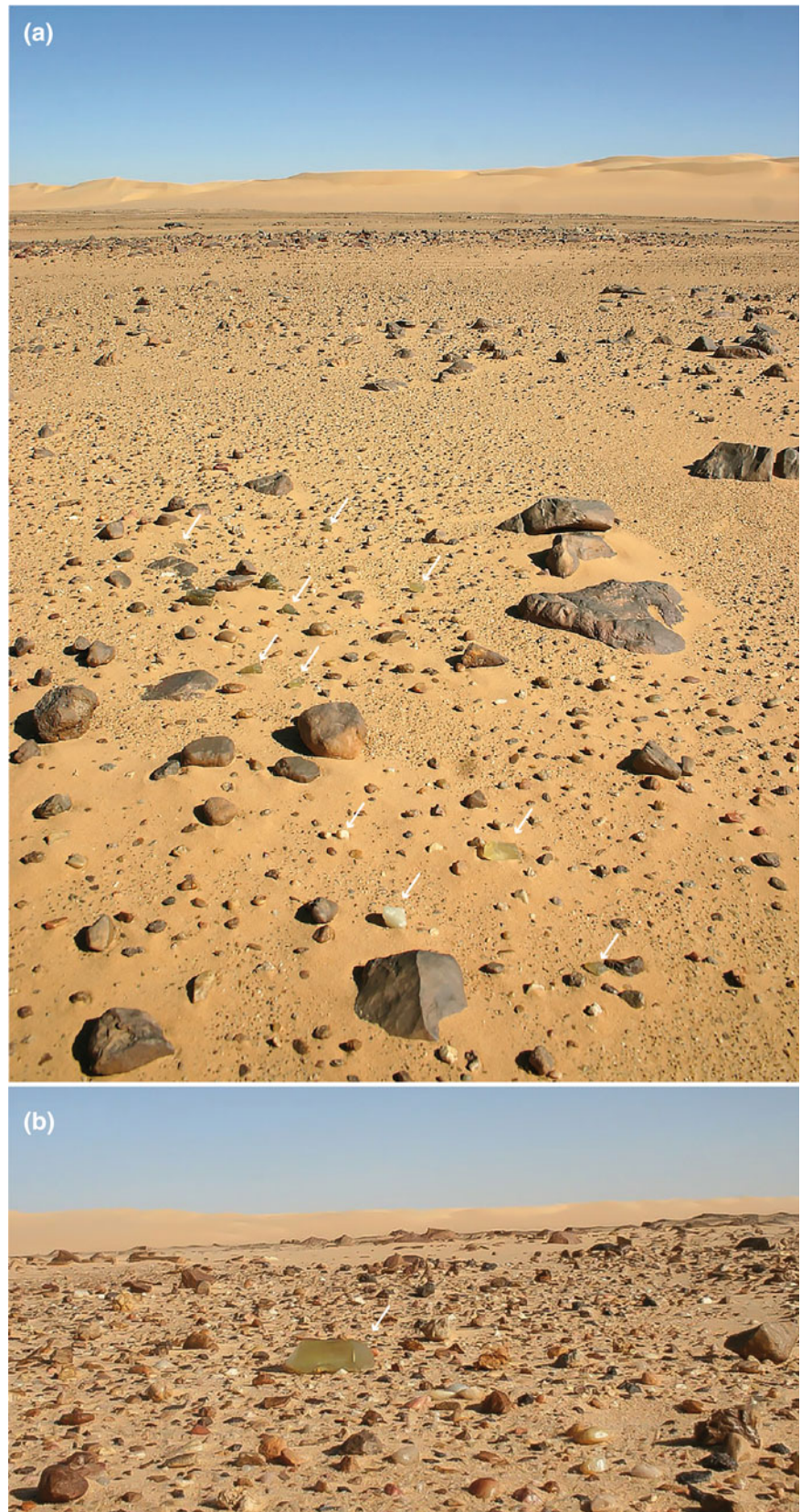
Fig. 11.8 The Kebira morphological feature. El-Baz and Ghoneim (2007) proposed that Kebira was an impact crater based on the analysis of satellite imagery (location map in Fig. 11.1). No crater is actually visible and no evidence of an impact origin has been found. Inset: the white dashed line traces the supposed crater outline (~ 31 km in diameter) according to El-Baz and Ghoneim (2007)

the order of 106 kg (Weeks et al. 1984) or 105 kg (Barakat et al. 1997). Accounting for the loss of material due to weathering, burial in the soil, and removal by primitive man who used LDG to make tools, the estimate of the original mass is 104 times greater (Weeks et al. 1984).

LDG specimens range in size from 30 cm to <1 cm across—biased by the limit of easy detection in the field. The largest specimen so far found has a mass of ~ 26 kg and is kept in the Museum National d’Histoire Naturelle in Paris, France (Diemer 1997). Although most specimens have irregular

Fig. 11.9 Libyan Desert Glass: Field occurrence.

a Centimeter-sized specimens of Libyan Desert Glass (arrowed) are found scattered in inter-dune corridors at the southern extension of the Great Sand Sea, Libyan Desert, southwestern Egypt (see Fig. 11.1 for location map). The surface of the inter-dune corridors consists of exposed sandstone bedrock (Cretaceous Nubia Formation), discontinuously covered by a colluvium-alluvium veneer of quartzose silt, sand and gravel (serir). **b** A closer view of one specimen in the field



shapes, many LDG samples are tabular reflecting the stratified character of the glass (Weeks et al. 1984). The dominant color of LDG is bright yellow–green, although varieties ranging from nearly colorless, to pale yellow, to grey-green are common too (Fig. 11.10). Most specimens are transparent to translucent, and some of them exhibit dark bands and schlieren. Some other specimens are opaque to milky white, with a cloudy appearance due to the conspicuous presence of vesicles. Clear and cloudy glass are arranged in layers in the largest tabular specimens. Oriented elongated vesicles and schlieren parallel to layering define flow textures. Scattered pale and dark millimeter-sized inclusions are visible to the naked eye in some specimens. The exposed surfaces are smooth, wind-polished with a glassy luster, whereas buried surfaces are irregular, rough and corroded by the dissolving action of soil moisture and ground water. Some pieces, namely flakes and hand-axes, show evidence of working by prehistoric man (Oakley 1952; Roe et al. 1982; Negro and Damiano-Appia 1992). LDG was also used in dynastic times as a valuable material; the scarab-shaped central motif of Tutankhamun's pectoral (14th C. BCE) was carved from LDG, according to the non-destructive refractive index analysis of De Michele (1998).

A number of mineralogical and petrographic studies (e.g. Kleinmann 1969; Barnes and Underwood 1976; Greshake et al. 2010, 2018; Swaenen et al. 2010; Cavosie and Koeberl 2019) have shown that LDG, although dominated by a glassy groundmass, does contain a variety of microscopic mineral inclusions including quartz, cristobalite, lechatelierite (pure silica glass), zircon and the thermal decomposition product of this latter mineral—baddeleyite, anatase, rutile, corundum, Al-rich orthopyroxene, and mullite (Figs. 11.10c, d). The occurrence, in particular, of lechatelierite, cristobalite, baddeleyite, decomposed Ti-magnetite and mullite testify to melting at temperatures in excess of 1670 °C. Such high formation temperatures are consistent with the emulsion textures observed under the transmission electron microscope (TEM) by Pratesi et al. (2002) in the dark bands, namely nanometer-scale spherules of glass enriched in Al, Fe and Mg indicative of liquid immiscibility with the surrounding silica glass. Granular zircons preserving evidence of reversion from former reidite were recently found in seven LDG specimens through electron back-scatter diffraction (EBSD) analysis (Cavosie and Koeberl 2019). This indicates the local attainment of pressure as high as 30 GPa.

The LDG is characterized by an extremely silica-rich composition. The SiO₂ content ranges from 96.5 to 99 wt%, with an average value of 98 wt% (Barnes and Underwood 1976; Fudali 1981; Koeberl 1997). Lithophile elements show inverse correlation with silica content, and the REE pattern is typical of upper continental crust materials (Koeberl 1997), consistent with a dominant quartz-rich sedimentary source. Further major and trace element analyses (Barrat et al. 1997),

Sr and Nd isotopic abundances (Schaaf and Müller-Sohnius 2002), and oxygen isotopic composition (Longinelli et al. 2011) indicate that the dominant parent material of LDG was a mature Cretaceous sandstone (or sands) most likely derived from the erosion of intrusive rocks of Pan African age (Neoproterozoic). Magna et al. (2011) noted that Libyan Desert Glass is characterized by a heavy Li signature ($d\ 7\text{Li} > 24.7\text{‰}$) and suggested that the LDG parent materials formed as alluvial-plain deposits in lacustrine and/or coastal marine environment during the Cretaceous. Fröhlich et al. (2013) studied LDG samples and locally occurring sediments collected during an archeological expedition in January 2006 by combined Fourier transform infrared spectroscopy and scanning e (SEM) microscopy. Their results suggested that the source rock of LDG was most probably quartz sand that had resulted from the weathering (loss of the cementing micro-quartz) of the Cretaceous sandstones of the Gilf Kebir Plateau with subsequent deposition in a high-energy, fluvial environment.

The composition of the dark bands is enriched in Cr (up to ~85 µg/g), Co (up to ~4 µg/g), Ni (up to ~55 µg/g), and Ir (up to ~6 ng/g), and their contents are also positively correlated with those of Fe and Mg (Murali et al. 1989; Rocchia et al. 1997; Koeberl 1997). This has been interpreted as a signature of a meteoritic component (Murali et al. 1989; Rocchia et al. 1997). In addition, Murali et al. (1997) showed that the siderophile element ratios in the dark bands of the LDG are consistent with a chondritic meteoritic component. Likewise, the significant PGE abundances detected in the dark bands by Barrat et al. (1997) and their CI normalized patterns revealed the presence of a chondritic component. Further evidence of the presence of a meteoritic component was provided by Re–Os isotope systematics of the dark bands (published in abstract form) by Koeberl (2000), a result later supported by the detection of crustal Sr and Nd abundances in LDG by Schaaf and Müller-Sohnius (2002) that are typical of intrusive rocks of Pan-African age and indicative of a negligible mantle component only.

Giuli et al. (2003) studied the iron oxidation state and coordination number in a LDG sample by means of iron K-edge high resolution X-ray absorption near-edge structure (XANES) spectroscopy. They found that iron is in the trivalent state in the pale silica glass, whereas it occurs in a more reduced state (bivalent) in the more Fe-rich dark bands. They suggested that some or most of the iron in these layers could be directly derived from the meteoritic projectile and that the LDG was not of terrestrial origin.

The age of the LDG was determined by the fission-track method. Storzer and Wagner (1977) obtained an Oligocene age of 29.4 ± 0.5 Ma, which was later confirmed by Bigazzi and de Michele (1997) with a result of 28.5 ± 0.8 Ma. Attempts to date LDG by means of the K–

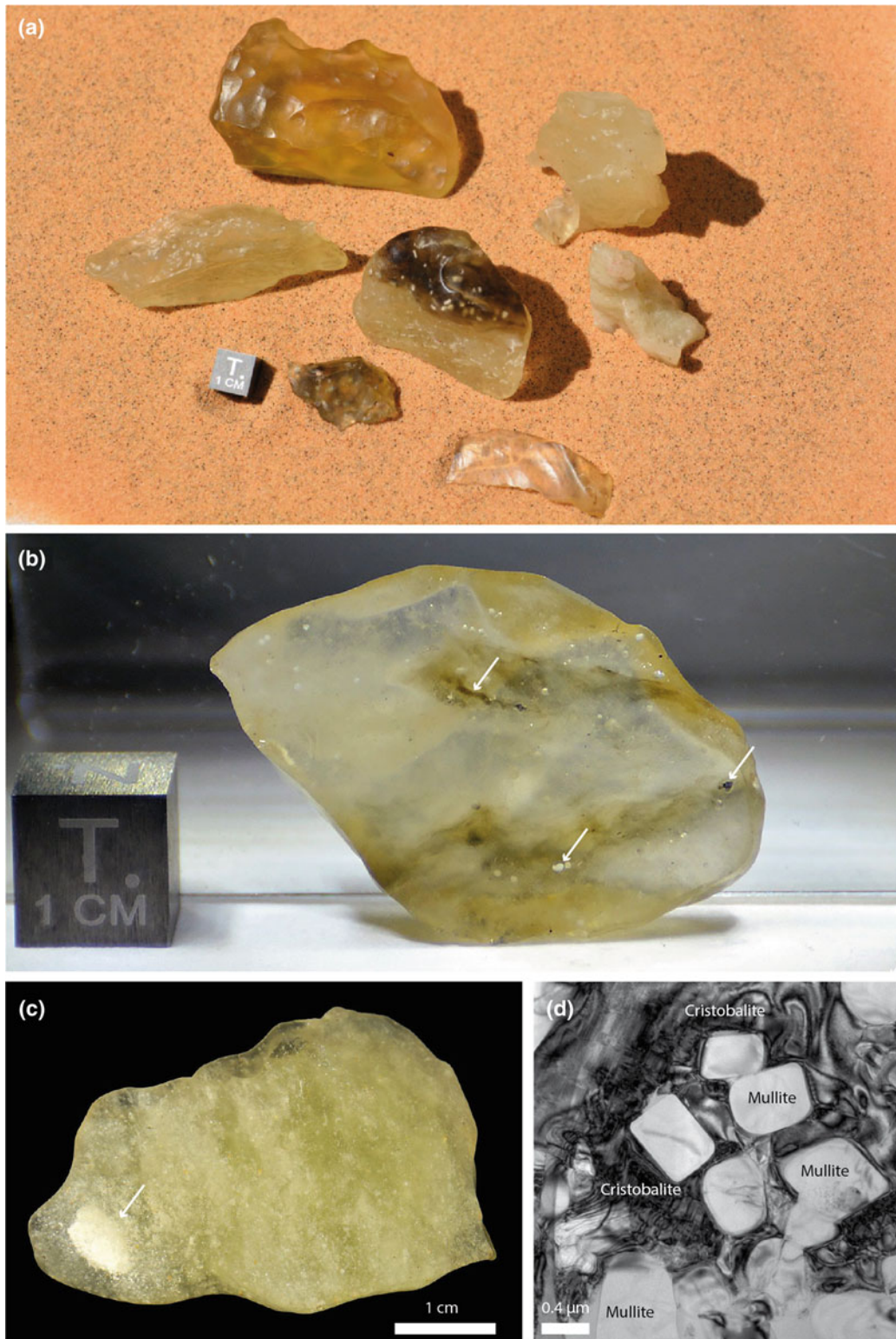


Fig. 11.10 Libyan Desert Glass: petrographic features. **a** A selection of Libyan Desert Glass specimens with varying color, transparency, amount of brown schlieren and degree of wind-blown polishing, including a flaked artifact of prehistoric age in the foreground (1 cm metal cube for scale). **b** An end-cut specimen of transparent to translucent glass bearing dark schlieren, and microscopic white and dark inclusions (arrowed). **c** A translucent to transparent specimen of Libyan Desert Glass with a large whitish inclusion (arrowed) bearing high-temperature assemblages of mullite plus cristobalite. **d** Transmission electron microscope image of a mullite-cristobalite bearing region in a whitish inclusion in Libyan Desert Glass (bright field image). Field images of Libyan Desert Glass specimens were kindly provided by Romano Serra (University of Bologna, Italy). The images of the whitish inclusions are courtesy of A. Greshake (Museum für Naturkunde, Berlin, Germany)

Ar method failed to provide reliable age data (Zahringer 1963; Horn et al., 1997; Matsubara et al. 1991).

There are several lines of evidence that LDG is an impact generated glass, although no source crater has been recognized so far. These include:

- i. The very high formation temperatures (in excess of ~ 1700 °C) and pressures (up to 30 GPa; Cavosie and Koeberl 2019) documented by the occurrence of mineral inclusions like lechatelierite, cristobalite, mulite, baddeleyite, Ti-magnetite decomposition products, and evidence for former reidite, respectively.
- ii. The presence of a chondritic geochemical signature in the dark bands.

In the past two possible source craters have been proposed: the 2-km-diameter BP impact crater and the 15 to 18-km-diameter Oasis impact structure, both located in southeastern Libya (Martin 1969; Underwood and Fisk 1980; Murali et al., 1988; Koeberl 1997; for detail about these structures: Reimold and Koeberl 2014). These structures are located ~ 150 km due W-SW of the LDG strewn field. The ages of these structures are essentially not known, as no datable materials have been identified at these structures. Based on a petrographic, geochemical, and Sr–Nd isotopic studies on a suite of target rock samples belonging to the Lower Cretaceous sandstone of the Nubian Sandstone from the BP and Oasis impact structures, Abate et al. (1999) concluded that the target rocks of the Libyan structures could represent the parent material for LDG. Later Schaaf and Müller-Sohnius (2002) determined Rb–Sr and Sm–Nd isotopic ratios from seven LDG samples and five associated sandstones from the LDG strewn field. They found Sr and Nd isotopic values for LDG similar to those of granitoid rocks from northeast Africa west of the Nile. They, thus, concluded that the LDG precursor material was a sandy matrix target material derived from a Precambrian crystalline basement, ruling out the Cretaceous sandstones of the Nubian Group as possible precursors for LDG.

To explain the lack of a source crater for LDG, some researchers have proposed that LDG was formed locally by the radiative heating/melting produced by the low-altitude airburst of a cometary or asteroidal object(s)—a process that might have been frequent in the collisional history of Earth (Wasson 2003; Boslough and Crawford 2008a, b). Indeed microscopic analysis of one of the five bedrock sandstone samples from the LDG strewn field studied by Kleinmann et al. (2001) and one out of a dozen studied by Koeberl and Ferrière (2019) revealed a wide range of deformation features in some of the constituent quartz grains, including crushing and fracturing, undulatory extinction, mosaicism, oriented cleavage, partial isotropization and multiple sets of planar deformation features. However, no trace of an impact

structure was found at or around this location, and the other studied rocks showed undisturbed textures without evidence of brecciation or shock features typical of impactites. This poses the question whether these rocks were actually the target rock in a hypervelocity impact, or whether the observed shock metamorphic features could predate the formation of these clastic sediments. In any case, evidence of former reidite precludes an origin of LDG by airburst alone (Cavosie and Koeberl 2019).

The definition of the formation mechanism of LDG is further complicated by two poorly constrained processes that might have significantly affected the spatial distribution of LDG and the survival of an impact structure, if there ever was one, since LDG formation in the Oligocene: mass-transport and erosion. Based on the variability of ^{10}Be and ^{26}Al exposure ages in twelve samples collected from representative sites of the LDG strewn field, Klein et al. (1986) concluded that individual fragments of glass had experienced different exposure histories, implying several major stages of redistribution of the glass within the past million years. According to the stratigraphic considerations by Giegengack and Underwood (1997), the area where LDG is found has undergone ~ 400 m of erosion since the formation of LDG ~ 28.5 million years ago.

Although nearly 85 years of geochemical studies have provided a wealth of information on the LDG glass and the nature of the source material, and an impact origin has been debated for essentially the same time, the actual impact scenario is still a matter of debate. In any case, the confirmation of the lack of substantial evidence for high shock pressure involved in the formation of LDG and having affected the country rocks, which would be a diagnostic feature of hypervelocity impacts, lends strong support to the low-altitude airburst model for the formation of LDG (Wasson 2003; Boslough and Crawford 2008a, b).

Kramers et al. (2013) reported on a dark, centimeter sized ($3.5 \times 3.2 \times 2.1$ cm), carbon-dominated, diamond-bearing rock fragment named “Hypatia” that had been found in the vicinity of the LDG strewn field at $25^{\circ}30' \text{ E}$, $25^{\circ}20' \text{ N}$ in 1996 (Barakat 2012). Based on Ar isotopic composition and non-terrestrial $\delta^{13}\text{C}$ values, these authors concluded that the fragment was most likely of extraterrestrial origin, and they hypothesized that it could be a remnant of a comet nucleus that exploded in air. Building on this hypothesis, Kramers et al. (2013) further speculated that Hypatia was a remnant of the airburst that generated the LDG. Through a comprehensive study of noble gases and nitrogen in several mg-sized samples, Avice et al. (2015) later confirmed the extraterrestrial nature of Hypatia. In particular, they:

- i. detected primordial noble gases (i.e., Q component) typical of various types of meteorites;

- ii. found a N isotopic composition consistent with C-components in meteorites, indicating that diamonds in Hypatia formed in space;
- iii. could not confirm detection of a noble gas presolar signature (i.e., the G component) that led Kramers et al. (2013) to speculate on a cometary origin of Hypatia;
- iv. determined a low concentration of cosmogenic ^{21}Ne , hinting at a parent object of at least a few meters in diameter but not necessarily large enough to have been able to create the LDG.

Recently, Belanyn et al. (2018) performed a mineralogical-petrographic study of a 4 g sample of Hypatia. They reported D and G bands in Raman spectra of disordered carbon with features similar to those observed in primitive solar system carbon materials, yet unlike any known cometary material. Therefore, although there is some evidence for an extraterrestrial origin of this anomalous and unique carbonaceous rock fragment, there is no evidence for a connection between Hypatia and the LDG—except that both these materials are derived from the same region. Hypatia, once its meteoritic origin is confirmed, would be one of the many meteorites found in the inter-dune corridors in the LDG strewn field (Fig. 11.1). Note also that Hypatia is not an official meteorite name. As reported by Belanyn et al. (2018), there is no type specimen curated in an acknowledged museum collection that would enable distribution of samples for research. This has thus far prevented proper classification of Hypatia as a meteorite, according to guidelines of the Nomenclature Committee of the Meteoritical Society.

11.3.4 Dakhleh Glass

In the Western Desert of Egypt, due south of the Libyan Plateau, the Dakhleh Oasis region (Figs. 11.1 and 11.11) preserves a rich history of habitation stretching back to over 400,000 years before the emergence of *Homo sapiens*. For this reason, this region has been the focus of intense (DOP) geo-archeological investigations by the Dakhleh Oasis Project since 1978 (Churcher and Mills 1999; Churcher et al. 1999). It was during the course of the Dakhleh Oasis Project field work in the 1980s and 1990s that a lag deposit of dark, glassy material on surface and within Pleistocene lacustrine deposits was discovered (Osinski et al. 2007): the so-called Dakhleh Glass—another unusual glass of proposed impact origin.

Subsequent reports of extensive field work and laboratory-based petrographic and geochemical analyses (Osinski et al. 2007, 2008) showed that the Dakhleh Glass lag deposit is composed of irregular and flattened masses of up to ~50 cm in size of vesicular glassy material. It occurs over an area of $\sim 40 \times \sim 10$ km, with ~140 individual locations

having been documented. Specimens of Dakhleh Glass are typically black in color when fresh, and greenish-grey when weathered (Fig. 11.11). Many specimens show impressions of leaves or plant stems. Petrographic analysis has shown that Dakhleh Glass consists of a highly vesicular, siliceous, glassy groundmass with variable contents of primary crystallites of clinopyroxene, with minor plagioclase, pyrrhotite microspherules, and calcite globules, as well as lithic and mineral clasts. Groundmass glass shows a variety of quench and flow textures: from transparent hypohyaline glass with compositional schlieren to opaque hypocrySTALLINE varieties. The glass composition (as determined by energy dispersive X-ray spectrometric system [EDS] and wavelength dispersive spectrometric system [WDS] analysis) is also variable, with silica contents ranging from ~50 to 70 wt%, and high concentrations of Ca and Al (CaO up to ~25 wt%, Al_2O_3 up to ~18 wt%), unlike any known volcanic glass. Clasts include rounded to sub-rounded quartz grains ~0.1–0.8 mm in diameter; pieces of silicified and/or fossilized plant matter; and angular fragments of fine-grained calcareous sedimentary rocks up to ~2 cm in size. In places, enclaves of silica-rich (90–100 wt% SiO_2) glass surround the quartz clasts. No evidence of shock metamorphism has been documented so far.

Based on archeological evidence from the DOP and preliminary ^{40}Ar – ^{39}Ar data, Osinski et al. (2007) suggested that the glass formed during the Middle Stone Age time of occupation. Subsequently, Renne et al. (2010) reported the results of several argon step-heating experiments, which yielded a preferred isochron age of 145 ± 19 ka, in keeping with the archeological constraints.

The origin of the Dakhleh Glass is debated. Osinski et al. (2007, 2008) suggested an impact melting origin, based on the non-volcanic chemical composition of the glass (particularly the high Al and Ca contents for a given silica content) and the absence of evidence of volcanism in that area are ruling out a volcanic origin. The high silica glass enclaves are interpreted as the products of melting of quartz clasts and related to lechatelierite inclusions in high temperature (>1700 °C) impact glasses, thus ruling out an origin through burning of vegetation or sediments rich in organic matter. Finally, the ~150 thousand year age of the glass excludes an anthropogenic origin. The lack of evidence of shock metamorphism and of an associated impact crater led Osinski et al. (2007, 2008) to speculate that Dakhleh Glass could have formed through radiative/convective heating of the surface during a large aerial burst in an event similar to that described by Wasson (2003) and Boslough and Crawford (2008a, b) and assumed for the origin of the LDG. In this view, the effects ~150 thousands years ago on the environment and inhabitants of the Dakhleh Oasis region would have been catastrophic. Recently, Roperch et al. (2017) proposed that natural fires were responsible for the formation of surface layers of silica glass in the Atacama



Fig. 11.11 The Dakhleh Glass (see Fig. 11.1 for location map). **a** Area of abundant masses of Dakhleh Glass lagged on the surface of Pleistocene lacustrine sediments; some large specimens are arrowed; hammer for scale. **b** Highly vesicular pumice-like Dakhleh Glass specimen. **c** Photomicrograph of a thin section of Dakhleh Glass showing an enclave of transparent, crystallite-free glass, within crystallite-rich darker glass. Images courtesy of G. Osinski (University of Western Ontario, Canada)

Desert (Chile), the so-called “Pica Glass”. In particular, they suggested that Pica Glass formed through the burning of organic-rich soils in dried-out grassy wetlands during climate oscillations between wet and dry periods. Although they did not find evidence of high temperature melting, they observed that Pica Glass and DG shared a number of structural and paleo-geographic features. They both have abundant plant imprints and they are confined to areas around oases. Roperch et al. (2017), thus, speculated that Pica Glass and Dakhleh Glass could share a similar origin by natural fires.

11.4 Meteorites: An Overview

Meteorites are interplanetary rock debris captured by Earth’s gravitational field and recovered at the Earth’s surface. Their size ranges from millimeters to few meters, i.e., large enough to survive atmospheric entry heating and small enough to be decelerated from their cosmic velocities (in excess of the Earth’s escape velocity of 11.2 km s^{-1}) through the Earth’s atmosphere and, therefore, survive impact against the Earth’s surface (e.g., Rubin and Grossman 2010). Their

hypervelocity passage through the upper Earth's atmosphere generates bright fireballs, explosions, detonations, and rumblings that have made them known since early human history (e.g., D'Orazio 2007). Object of veneration and popular superstition and recurring element in myths up until the 18th century CE, meteorites are for modern science a natural laboratory to investigate the origin and evolution of the solar system. Meteorites are in fact rock samples of a large variety derived from a range of solar system bodies, with a large variety of geological histories: from primitive minor bodies like the asteroids, to more evolved planetary bodies like Mars and the Moon (e.g., Chambers 2006). The cosmochemical and geochemical study of their physico-chemical properties thus allows investigation of the ~4.6 billion year long sequence of processes through which an interstellar molecular cloud of gas and dust became a system of planets and other minor bodies orbiting around the Sun (e.g., McSween et al. 2006; Russell et al. 2006).

Meteorites have traditionally been distinguished into three broad categories—stones, irons, and stony-irons based on the relative proportions of silicate minerals and metallic iron–nickel. Modern classification schemes group meteorites into homogeneous classes according to their structure, chemical and isotopic composition, and mineralogy (e.g., Krot et al. 2014). The most abundant meteorites in our collection (>99% of the total) are impact debris from collisions between asteroids orbiting between Mars and Jupiter. Asteroids are “fossil bodies” of the planet building era. Unlike the geologically more evolved terrestrial, Martian, and lunar rocks, asteroidal meteorites uniquely contain minerals that formed before the solar system, and during the growth and differentiation of planetesimals and planets from the disk of dust and gas around the Sun (known as the ‘solar nebula’) within the first few tens of million years of solar system evolution. Amongst asteroidal meteorites, ~85% are chondrites, primitive rocks that have elemental compositions similar to that of the Sun (e.g., Scott and Krot 2014). They sample asteroids that did not experience melting, although evidence of thermal metamorphism and aqueous alteration in some chondrite classes attests to some heating in bodies with anhydrous and hydrous compositions, respectively. About 14% of meteorites arriving on Earth consist of differentiated materials (McCoy et al. 2006). These are meteorites known under the names of achondrites, irons, and stony-irons, which derive from asteroids that underwent melting and differentiation into metallic iron cores and silicate mantles, like the ~500-km-diameter asteroid 4Vesta which can be associated with one group of achondrites denominated HED (the howardite-eucrite-diogenite group). Rare stony meteorites blasted off the surfaces of the Moon and Mars by impact events comprise less than 1% of the total known meteorites. The 340 lunar meteorites, or lunaites, to date present in our collections represent a valuable extension to

the Apollo and Luna sampling of the Moon's surface debris, providing additional clues into the geological evolution of the lunar crust, the formation of the Earth-Moon system, and the intense cosmic bombardment that affected the inner solar system bodies during the first few hundred million years of its evolution (e.g., Warren and Taylor 2014). The 290 Martian meteorites are the only rock samples from planet Mars available in our laboratories (e.g., McSween and McLennan 2014). They include basalts and cumulates formed from basaltic magmas, and which have revealed that planetary differentiation on Mars occurred ~4.5 billion years ago, probably during accretion, and that magmatism extended through the period from 1.3 Ga to 180 Ma. These meteorites have also provided insight into the geological history of the planet, including the composition of its Fe-rich mantle, as well as atmosphere composition and subsurface water circulation in response to changes in the climatic evolution of Mars (e.g., Bridges et al. 2001; Chennaoui Aoudjehane et al. 2012).

Over 59,000 meteorites, of up to 60 t in mass, with many in the 10–100 g range, are listed in The Meteoritical Bulletin Database (<https://www.lpi.usra.edu/meteor/metbull.php>), the authoritative source of information on approved meteorites, which is provided by the Meteoritical Society. Of these, 1310 meteorites were seen to fall (and are known as ‘falls’).

The oldest meteorite fall, for which material is still available for science, is the meteorite of Ensisheim (Alsace, France, 1492). Since the late 1950s, the fall of a few meteorites have been detected through networks of camera stations (e.g., the European Camera Network in central Europe, Oberst et al. 1998; Prairie Meteorite Network in the mid-western United States, McCrosky et al. 1971; The Meteorite Observation and Recovery Project in western Canada, Halliday et al. 1978; the Australian Desert Fireball Network in Western Australia, Bland, 2004) designed to track meteoroids entering the atmosphere, determine pre-entry orbits, and recover meteorites. By far most of the others are the tens of thousands of ‘finds’ recovered from hot and cold deserts over the last 50 years. Hamada (nearly bare bedrock-desert) and serir (gravel/pebble-desert) type hot desert surfaces in the Sahara, Atacama, and Nullarbor Plain, and the many blue ice fields on the Antarctic plateau are the most productive terrains for the collection of meteorites on Earth—a treasure-trove for planetary science.

11.5 The Meteorite Record of Egypt

The Meteoritical Bulletin Database to date (June 2018) lists 78 meteorites from Egypt (Table 11.1). Seventy-six are finds and two are observed falls: Nakhla (1911) and Sinai (1916). With the exception of the iron meteorite Gebel Kamil from Kamil Crater with a total recovered mass of ~1.7 t,

Table 11.1 Egyptian meteorites (listed alphabetically; Meteoritical Bulletin Database; accessed September 2018)

Name	Abbreviation	Fall	Year	Place	Type	Mass	Name	Abbreviation	Fall	Year	Place	Type	Mass
Abu Moharek			1997	Al Wadi al Jadid, Egypt	Ordinary chondrite H4	4.5 kg	Great Sand Sea 033	GSS 033		2006	Al Wadi al Jadid, Egypt	Ordinary chondrite L5	80.1 g
Al Alamayn			2005	Marsa Matruh, Egypt	Ordinary chondrite H5	13.3 g	Great Sand Sea 034	GSS 034		2006	Al Wadi al Jadid, Egypt	Ordinary chondrite L5/6	7.7 g
Aswan			1955	Al Wadi al Jadid, Egypt	Iron, IAB-ung	12 kg	Great Sand Sea 035	GSS 035		2007	Al Wadi al Jadid, Egypt	Ordinary chondrite H5/6	40.9 g
Birkat Aghurmi 001			2012	Marsa Matruh, Egypt	Ordinary chondrite L6	1666 g	Great Sand Sea 036	GSS 036		2007	Al Wadi al Jadid, Egypt	Ordinary chondrite H5	128.9 g
El Bahrain			1983	Marsa Matruh, Egypt	Ordinary chondrite L6	14 kg	Great Sand Sea 037	GSS 037		2007	Al Wadi al Jadid, Egypt	Ordinary chondrite H4	66.9 g
El Faiyum			1993	Al Fayyum, Egypt	Ordinary chondrite H5	73.5 g	Great Sand Sea 038	GSS 038		2007	Al Wadi al Jadid, Egypt	Ordinary chondrite H5	146 g
El Qoseir			1921	Al Bahr al Ahmar, Egypt	Iron, ungrouped	2.41 kg	Great Sand Sea 039	GSS 039		2007	Al Wadi al Jadid, Egypt	Ordinary chondrite H5	128.6 g
El-Quss Abu Said			1999	Al Wadi al Jadid, Egypt	CM2	53.1 g	Great Sand Sea 040	GSS 040		2010	Al Wadi al Jadid, Egypt	Ordinary chondrite LL5	15 g
El-Shaikh Fadl 001	ESF 001		2010	Al Bahr al Ahmar, Egypt	Ordinary chondrite H5	476 g	Great Sand Sea 041	GSS 041		2010	Al Wadi al Jadid, Egypt	Ordinary chondrite H5	6.5 g
El-Shaikh Fadl 002	ESF 002		2010	Al Bahr al Ahmar, Egypt	Ordinary chondrite H5	806 g	Isna			1970	Al Wadi al Jadid, Egypt	CO3.8	23 kg
El-Shaikh Fadl 003	ESF 003		2009	Al Bahr al Ahmar, Egypt	Ordinary chondrite H4	73 g	Kharga			2000	Marsa Matruh, Egypt	Iron, IVA	1040 g
El-Shaikh Fadl 004	ESF 004		2009	Al Bahr al Ahmar, Egypt	Ordinary chondrite L5	8.01 kg	Marsa Alam			2012	Al Bahr al Ahmar, Egypt	Ordinary chondrite H5	69 g
El-Shaikh Fadl 005	ESF 005		2010	Al Bahr al Ahmar, Egypt	Ordinary chondrite L-mr*	538 g	Marsa Alam 002	MA 002		2013	Al Bahr al Ahmar, Egypt	Ordinary chondrite H5	336 g
El-Shaikh Fadl 006	ESF 006		2010	Al Bahr al Ahmar, Egypt	Ordinary chondrite H5	52.2 g	Marsa Alam 003	MA 003		2014	Al Bahr al Ahmar, Egypt	Ordinary chondrite H5	10.7 g
El-Shaikh Fadl 007	ESF 007		2010	Al Bahr al Ahmar, Egypt	Ordinary chondrite L5	8.2 kg	Marsa Alam 004	MA 004		2014	Al Bahr al Ahmar, Egypt	Ordinary chondrite L5-6	37.6 g
El-Shaikh Fadl 008	ESF 008		2010	Al Bahr al Ahmar, Egypt	Ordinary chondrite H5	66.5 g	Marsa Alam 005	MA 005		2014	Al Bahr al Ahmar, Egypt	Ordinary chondrite L5	314 g
El-Shaikh Fadl 009	ESF 009		2010	Al Bahr al Ahmar, Egypt	Ordinary chondrite H5	56.3 g	Marsa Alam 006	MA 006		2013	Al Bahr al Ahmar, Egypt	Ordinary chondrite H3-5	97 g
El-Shaikh Fadl 010	ESF 010		2010	Al Bahr al Ahmar, Egypt	Ordinary chondrite H5	75.7 g	Marsa Alam 007	MA 007		2013	Al Bahr al Ahmar, Egypt	Ordinary chondrite H3.6-4	90.5 g
Gebel Kamil			2009	Al Wadi al Jadid, Egypt	Iron, ungrouped	1.6 t	Marsa Alam 008	MA 008		2015	Al Bahr al Ahmar, Egypt	Ordinary chondrite L6	4.45 kg
Great Sand Sea 001	GSS 001		1991	Al Wadi al Jadid, Egypt	Ordinary chondrite L6	130 g	Marsa Alam 009	MA 009		2015	Al Bahr al Ahmar, Egypt	Ordinary chondrite H6	4.33 kg
Great Sand Sea 002	GSS 002		1991	Al Wadi al Jadid, Egypt	Ordinary chondrite L6	135 g	Marsa Alam 010	MA 010		2015	Al Bahr al Ahmar, Egypt	Ordinary chondrite H5	165.3 g

(continued)

Table 11.1 (continued)

Name	Abbreviation	Fall	Year	Place	Type	Mass	Name	Abbreviation	Fall	Year	Place	Type	Mass
Great Sand Sea 003	GSS 003		1991	Al Wadi al Jadid, Egypt	Iron	110 g	Marsa Alam 011	MA 011		2015	Al Bahr al Ahmar, Egypt	Ordinary chondrite L5	75.6 g
Great Sand Sea 004	GSS 004		1994	Al Wadi al Jadid, Egypt	Ordinary chondrite LL6	580 g	Marsa Alam 012	MA 012		2014	Al Bahr al Ahmar, Egypt	Ordinary chondrite H4	3.3 g
Great Sand Sea 005	GSS 005		1995	Al Wadi al Jadid, Egypt	Ordinary chondrite L6	80 g	Marsa Alam 013	MA 013		2015	Al Bahr al Ahmar, Egypt	Ordinary chondrite H6	168 g
Great Sand Sea 006	GSS 006		1995	Al Wadi al Jadid, Egypt	Ordinary chondrite L6	45 g	Marsa Alam 014	MA 014		2015	Al Bahr al Ahmar, Egypt	Ordinary chondrite L5	2.48 g
Great Sand Sea 007	GSS 007		1996	Al Wadi al Jadid, Egypt	Ordinary chondrite H6	1450 g	Marsa Alam 015	MA 015		2015	Al Bahr al Ahmar, Egypt	Ordinary chondrite H4	30.6 g
Great Sand Sea 008	GSS 008		1996	Al Wadi al Jadid, Egypt	Ordinary chondrite LL3-6	450 g	Marsa Alam 016	MA 016		2015	Al Bahr al Ahmar, Egypt	Ordinary chondrite H4	53.9 g
Great Sand Sea 009	GSS 009		1996	Al Wadi al Jadid, Egypt	Ordinary chondrite H5	414 g	Marsa Alam 017	MA 017		2015	Al Bahr al Ahmar, Egypt	Ordinary chondrite H6	115.1 g
Great Sand Sea 019	GSS 019		1999	Al Wadi al Jadid, Egypt	Ordinary chondrite LL6	12 kg	Marsa Alam 018	MA 018		2015	Al Bahr al Ahmar, Egypt	Ordinary chondrite H5	3.78 g
Great Sand Sea 020	GSS 020		2000	Al Wadi al Jadid, Egypt	Ordinary chondrite H	5.42 kg	Marsa Alam 019	MA 019		2015	Al Bahr al Ahmar, Egypt	Ordinary chondrite H6	291 g
Great Sand Sea 021	GSS 021		2002	Marsa Matruh, Egypt	Ordinary chondrite L5	1416 g	Minqar Abd el Nabi			1992	Marsa Matruh, Egypt	Ordinary chondrite H6	362 g
Great Sand Sea 022	GSS 022		1994	Al Wadi al Jadid, Egypt	Ordinary chondrite H6	0.9 g	Mut			2003	Al Wadi al Jadid, Egypt	Ordinary chondrite H5	1800 g
Great Sand Sea 023	GSS 023		1996	Al Wadi al Jadid, Egypt	Ordinary chondrite H5	1.5 g	Nakhla		Y	1911	Al Buhayrah, Egypt	Martian (nakhlite)	10 kg
Great Sand Sea 024	GSS 024		1996	Al Wadi al Jadid, Egypt	Ordinary chondrite H5	7.8 g	Nova 012			2010	Egypt	Ordinary chondrite H5	266 g
Great Sand Sea 025	GSS 025		2005	Al Wadi al Jadid, Egypt	Ordinary chondrite L5	10.9 g	Quarat al Hanish			1979	Al Wadi al Jadid, Egypt	Iron, IAB-sHL	593 g
Great Sand Sea 026	GSS 026		2007	Marsa Matruh, Egypt	Ordinary chondrite H6	100 g	Sinai		Y	1916	Al Isma'iliyah, Egypt	Ordinary chondrite L6	1455 g
Great Sand Sea 030	GSS 030		2006	Al Wadi al Jadid, Egypt	Ordinary chondrite H6	51.3 g	Siwa			1994	Marsa Matruh, Egypt	Ordinary chondrite L5-6	36 g
Great Sand Sea 031	GSS 031		2006	Al Wadi al Jadid, Egypt	Ordinary chondrite H5	62.3 g	Thamaniyat Ajras			2016	Al Wadi al Jadid, Egypt	Ordinary chondrite L6	866 g
Great Sand Sea 032	GSS 032		2006	Al Wadi al Jadid, Egypt	Acapulcoite	8.3 g							

Egyptian meteorites range in mass from just a few grams to less than 10 kg, for a total recovered mass of ~ 1725 kg. Besides 67 ordinary chondrites, the most abundant group of meteorites in the world's collection, there are a number of rare meteorites amongst the Egyptian collection. They include one Martian meteorite, two carbonaceous chondrites,

one acapulcoite, and seven iron meteorites. The Martian meteorite is named Nakhla (Fig. 11.12), and it is surely a most remarkable specimen as it is one of the rare samples in the world's collections from the surface of planet Mars. As reported by the Meteoritical Bulletin Database, on 28 June 1911, at 9:00 a.m., a shower of multiple fragments of the

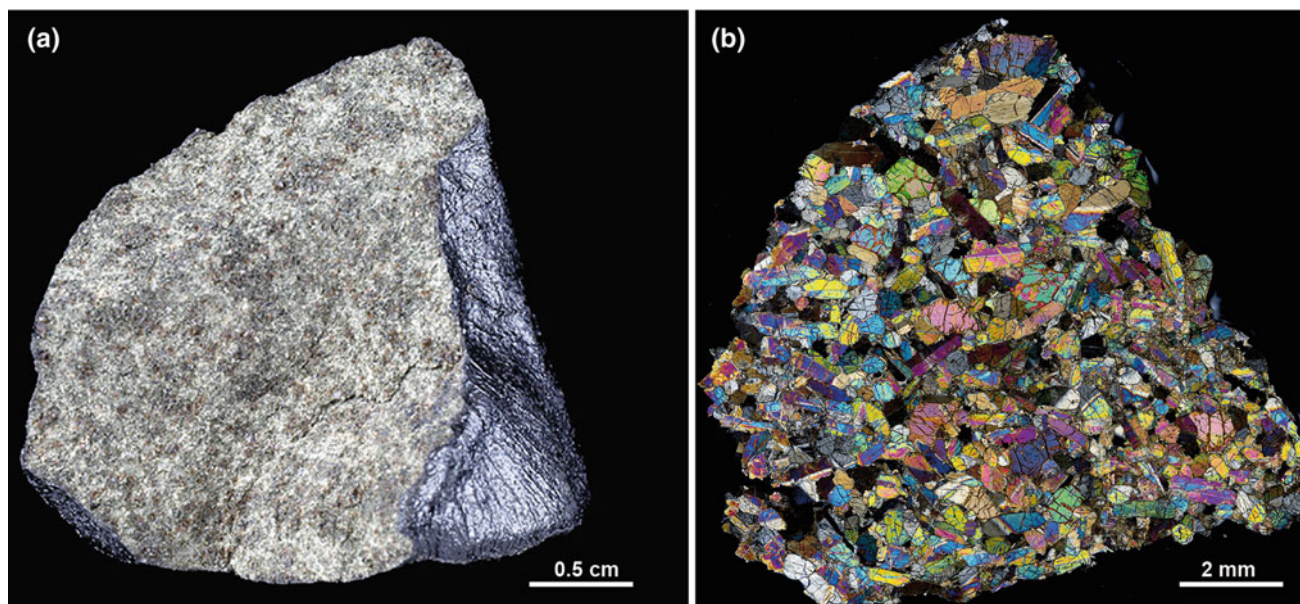


Fig. 11.12 The Nakhla martian meteorite. **a** A specimen of the Nakhla meteorite shower that fell in Egypt on June 28th, 1911 near the village of El Nakhla. The specimen, broken off for curatorial purposes, shows a shiny black fusion crust and a crystalline igneous textured interior. **b** Optical micrograph (crossed polars) of a petrographic thin section of the same specimen showing that Nakhla is a clinopyroxenite, dominated by augite with less abundant Fe-rich olivine, plagioclase, K-feldspars, Fe–Ti oxides, FeS, chalcopyrite and a hydrated alteration phase. Images courtesy of Sara Russell and Natashia Almeida (Natural History Museum, London, UK). Photo credit: © The Trustees of the Natural History Museum, London

Nakhla meteorite was seen to fall in the hamlets surrounding the village of El-Nakhla, El-Bahariya in Egypt, near Alexandria. Dr. W. F. Hume, at the time Director of the Geological Survey of Egypt, personally visited the site and collected both the evidence of eyewitnesses of the fall and about a dozen specimens varying in weight from 1813 to 20 g, for a total recovered mass of ~ 10 kg. Nakhla is a clinopyroxenite with a crystallization age of ~ 1.3 billion years before present (Treiman 2005)—a cornerstone specimen for understanding the igneous process on Mars (Bridges and Warren 2006; McSween and McLennan 2014).

With the exception of a minority of incidental finds ($n = 18$; $\sim 25\%$ of the total number of finds), the majority of the Egyptian finds ($n = 58$; $\sim 75\%$) were recovered over the last 30 years from three regions defined as dense collection areas (DCAs; i.e., stable geological surfaces with the potential of yielding large accumulations of meteorites, namely ~ 0.01 to ~ 10 meteorites per square kilometer; Abu Aghreb et al. 2003; Gattacceca et al. 2011) in The Meteoritical Bulletin, namely the El-Shaik Fedl, Great Sand Sea and Marsa Alam fields (Figs. 11.1 and 11.13). The great majority of these meteorites were recovered by private collectors. As a consequence, little information is available on the geological characteristics of the collection surfaces and, thus, on the actual potential yield of those. Only few meteorites from the Great Sand Sea dense collection area were recovered during scientific expeditions carried out by

Italian-Egyptian parties involved in the study of the Libyan Desert Glass during the early 1990s (e.g., Barakat et al. 1996; Barakat 1991). Even in this case, little information on the circumstances of the finds and on the meteorite collection surfaces has been reported, except that they were found in the inter-dune deflation corridors dominated by quartzose gravel, like the specimens of Libyan Desert Glass. The number of meteorites found in these three dense collection areas is, however, a small fraction of the hundreds-to-thousands of meteorites found in other desert areas in the Libyan and Algerian Sahara (e.g., the Acfer, Dar al Gani and Hamadah al Hamra DCAs; e.g., Schlüter et al. 2002), in the Atacama (e.g., the San Juan and El Medano DCAs; e.g., Gattacceca et al. 2011; Hutzler et al. 2016), and in Oman and Saudi Arabia (e.g., Dhofar; Al-Kathiri et al. 2005), and the actual meteorite accumulation potential of these Egyptian sites should be properly assessed.

11.6 Meteorites in the Archeological Record of Ancient Egypt

Amongst the earliest iron artifacts of human history, there are a number of Ancient Egyptian iron artifacts that predate the iron age, and for which a meteoritic origin has been recently documented through non-destructive geochemical analysis. These artifacts include nine small iron beads dated

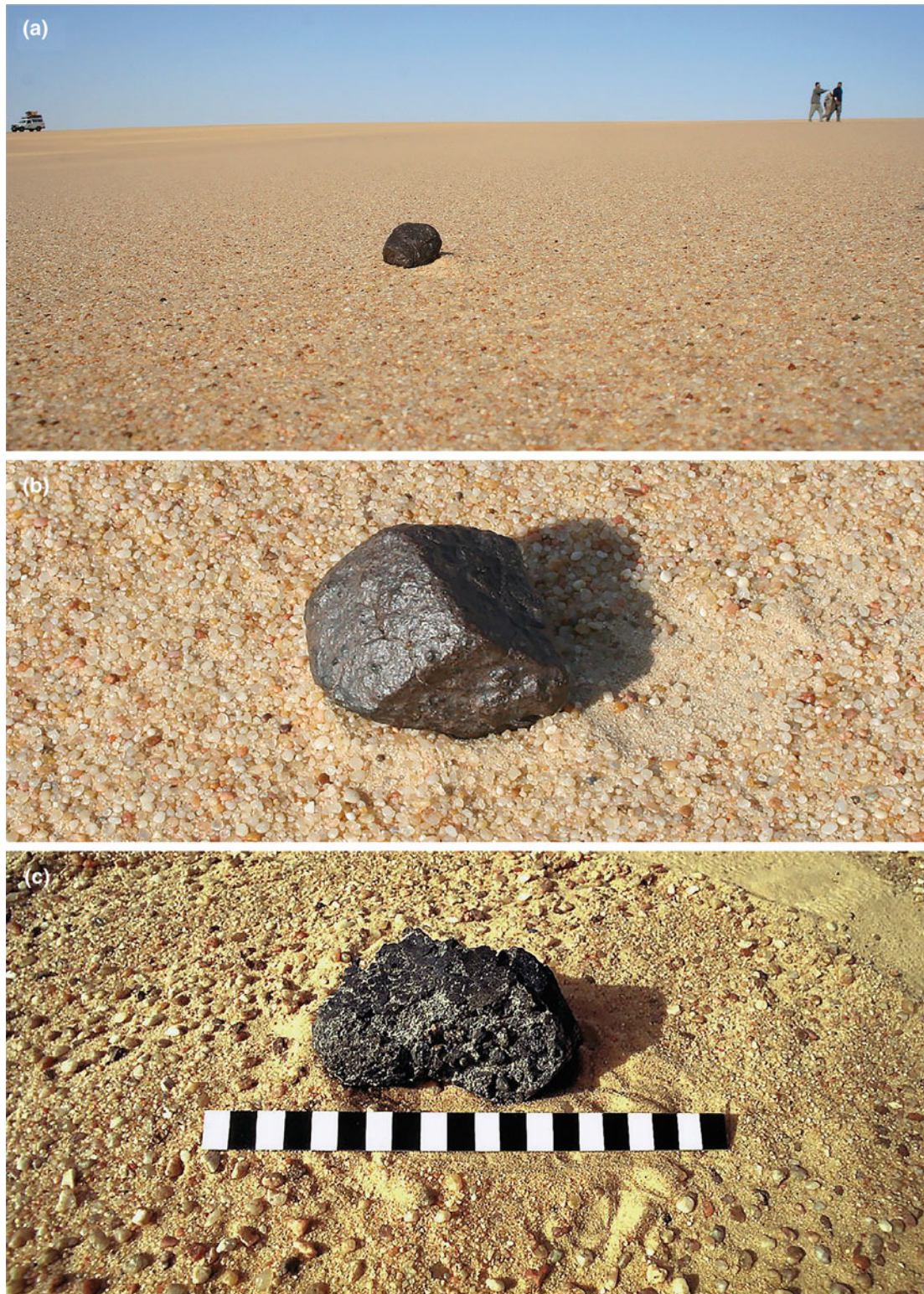


Fig. 11.13 Meteorite finds from the Dense Collection Area denominated Great Sand Sea (GSS). See Fig. 11.1 for the location of the GSS area. A) Field photo of meteorite GSS 026 ($28^{\circ}11'21''$ N, $25^{\circ}37'18''$ E), a H6 ordinary chondrite with a fairly oxidized (weathered) fusion crust sitting on the pale surface of an interdune deflation corridor dominated by well-sorted quartzose gravel (serir). B) A close-up view of the same meteorite in the field. C) Field photo of the relatively fresh GSS 004 LL6 ordinary chondrite ($25^{\circ}35'35''$ N, $25^{\circ}31'40''$ E) showing some erosion of the black fusion crust. The black fusion crust, resulting from surface ablation during atmospheric entry heating, is a macroscopic diagnostic feature for the identification of meteorites in the field. Meteorites were collected during the Italian-Egyptian expeditions for the study of the Libyan Desert Glass carried out in between 1991 and 1996. Images courtesy of R. Serra (Universita di Bologna, Italy)



Fig. 11.14 Meteoritic iron in the history of Ancient Egypt. **a** Optical image (left) of a bead from a tomb in Gerzeh (Egypt) and dated about 3200 BCE made of meteoritic iron, and a Computer Tomography cross-section view (right) revealing how the bead was carefully hammered into thin sheets (Johnson et al. 2013; Rehren et al. 2013). The bead is ~ 2 cm in length and 3–8 mm in diameter. Images courtesy of Diane Johnson (Open University, UK). **b** The iron dagger of King Tutankhamun (14th C. BCE) with its gold sheath (Carter no. 256K, JE 61585). The full length of the dagger is 34.2 cm (modified after Comelli et al. 2016)

to ~ 3200 BC from two prehistoric burials discovered in Gerzeh, 70 km south of Cairo, northern Egypt, by British archeologist Gerald Wainwright in 1911 (Johnson et al. 2013; Rehren et al. 2013), and the iron blade of one of the two daggers found in the wrappings of King Tutankhamun (14th C. BCE) by British archeologist Howard Carter in 1925 (Comelli et al. 2016; Fig. 11.14).

Through a combination of scanning electron microscopy and micro X-ray microcomputer tomography, Johnson et al. (2013) showed that the microstructural and chemical analysis of a Gerzeh iron bead strung on a necklace from tomb 67 is consistent with a cold-worked iron meteorite. This finding was later confirmed by Rehren et al. (2013) by neutron and X-ray methods, which revealed substantial amounts of Ge (30–100 $\mu\text{g/g}$), 6–9 wt% Ni and 0.4–0.5 wt% Co. These results reveal the status of meteoritic iron as a valuable material for the production of precious objects, and document that already in the fourth millennium BC metalworkers had mastered the smithing of meteoritic iron.

The composition of the iron blade of King Tutankhamun's dagger (Fe plus 10.8 wt% Ni and 0.58 wt% Co), determined through portable X-ray fluorescence spectrometry, strongly supports its meteoritic origin (Comelli et al. 2016). In order to investigate whether known iron meteorites within the ancient Egyptian trade sphere could be linked to

the studied blade, Comelli et al. (2016) compared this composition with those of the twenty known meteorites found in the region from the central-eastern Sahara to the Arabic Peninsula, Mesopotamia, Iran, and Eastern Mediterranean area, but no good match was found. This work confirmed that ancient Egyptians attributed great value to meteoritic iron for the production of fine ornamental or ceremonial objects. Furthermore, the high manufacturing quality of Tutankhamun's dagger blade, in comparison with other simple-shaped meteoritic iron artifacts, documents a significant mastery of ironworking in Tutankhamun's time.

11.7 Outlook

The work carried out at Kamil Crater (e.g., Folco et al. 2010, 2011) and in the so-called Gilf Kebir Crater Field (Paillou et al. 2006; Orti et al. 2008) has shown the importance of satellite image analysis in the identification of potential new impact craters, particularly in desert areas characterized by exceptional rock exposures. It has also shown the importance of field work in confirming the impact origin, through the identification of diagnostic features including traces of the impactor, and meso-to-microscopic shock metamorphic features (e.g., French and Koeberl 2010). The combination

of these two methodological approaches is a fundamental prerequisite for the identification of new impact structures.

Due to its extraordinary state of preservation, the 45-m-diameter, less than 5,000 years old Kamil Crater (Fig. 11.3) is a type-structure for small-scale meteorite impacts on Earth (Folco et al. 2011). Field and laboratory work has documented that Kamil is a natural laboratory for investigating processes and products generated by the hypervelocity impact of small meteoritic bodies. Advancements in the field of small-scale impact cratering are expected from the integration of ground truth, numerical models, and laboratory hypervelocity impact experiments (e.g., Kenkmann et al. 2013; Folco et al., 2018; Hamann et al. 2018; Wilk et al., 2018; Cavosie and Folco, 2018).

The large number of specimens of Gebel Kamil (the meteorite that formed Kamil Crater) which were smuggled out of Egypt and put on the worldwide market by private collectors document that the integrity of Kamil Crater is at serious risk. Egyptian geosocieties and legislative bodies should devise strategies for the conservation of this unique location and consider this structure as a resource not just for science, but also for tourism and education. Kamil is indeed located in a remote area of the Egyptian desert, yet it is close to the Gilf Kebir National Park, which is an extraordinary tourist attraction. Virtuous examples around the world of protected impact structures utilized for geotourism and educational purposes include—for instance—the Barringer crater (Arizona) or the Ries crater in the GeoPark Ries (Germany). The latter also features a unique museum in the City of Nordlingen, dedicated to the education about the Ries impact and impact cratering in general.

Although the Libyan Desert Glass and the Dakhleh Glass are silicate glasses of suggested impact origin (e.g., Barrat et al. 1997; Koeberl 2000; Osinski et al. 2007), no associated impact craters have been found yet. The study of these glasses has, thus, been instrumental for developing models for the formation of extended surface layers of unusual silicate glass by processes other than impact cratering, including a low-altitude airburst for the Libyan Desert Glass (Wasson 2003; Boslough and Crawford 2008a, b) and natural fires for the Dakhleh Glass (Roperch et al. 2017). The recent finding of evidence for high-pressures in some LDG specimens (Cavosie and Koberel 2019) requires a crater-forming event and that airburst alone could not be responsible for the formation of LDG.

Our knowledge of the origin and evolution of the solar system stems from the effective synergy between astronomical observations, space missions, astrophysical modeling and the cosmochemical study of thousands of meteorites (Russell, 2018). The larger the number of meteorites in our collections, the larger the chance of identifying new extraterrestrial rock types carrying new information about the processes that led to the formation of the solar system. This motivates the interest of

the planetary science community in continuing the search for, and collection of, meteorites. The vast extensions of the hamada and serir type surfaces of the Egyptian desert plateaus are thus of great interest for systematic search for meteorites (Fig. 11.13). About 75% of the meteorites in the Egyptian collection were found in three dense collection areas (DCAs) mainly by private collectors, with little information on the characteristics of the collection surfaces being recorded. Therefore, the potential of these areas to yield high concentrations of meteorites should be investigated properly through field and laboratory work, taking advantage of the experience of other research groups in other desert areas in the Sahara, Atacama, Oman deserts, etc. (e.g., Schlüter et al. 2002; Hutzler et al. 2016). Data about terrestrial ages (i.e., the time since the fall) of the meteorites found in these DCAs and weathering style/rates would be relevant to assess the survival time of meteorites in these environments and the collection time window, and thus the local evolution of the climate (e.g., Bland et al. 1996; Jull 2006).

Fireball camera network projects are designed to track meteoroids entering the atmosphere, determine pre-entry orbits, and pinpoint fall positions for recovery (e.g., Oberst et al. 1998; Bland, 2004). These networks provide a wealth of information to the astronomical and planetary science community by linking pristine planetary materials to their source regions in the solar system (e.g., Bland et al. 2009). The vast desert lands of the Egyptian territory (~1 million square km), with virtually no vegetation for over 95% of their entire extension, should be assessed for the installation of fireball camera networks.

The Geological Museum in Cairo hosts a small yet valuable collection of meteorites, including a specimen of the Martian meteorite Nakhla (Fig. 11.12) and ~700 kg of the iron meteorite Gebel Kamil (~600 kg of shrapnel and the main mass of the regmaglypted individual featured in Fig. 11.4c). Systematic search for meteorites should be conducted by Egyptian research institutes in the Egyptian deserts to enrich this collection. All this would make great material for public exhibits. The scientific value and the societal impact of the study and curation of meteorites are widely accepted in today's scientific community (Baratoux et al. 2017).

Non-destructive compositional analyses of the Gerzeh iron beads (~3000 BCE; Johnson et al. 2013; Rehren et al. 2013) and of Tutankhamun's dagger blade (XIV C. BCE; Comelli et al. 2016) (Fig. 11.14) revealed that two pre-iron age Ancient Egyptian iron artifacts are made of meteoritic iron. The implications of such studies extend beyond this specific pre-iron age Egyptian use of iron, if we consider that the working of metal has played a crucial role in the evolution of human civilization. Non-destructive compositional analysis of other time-constrained ancient iron artifacts present in world collections are, thus, expected to provide significant insight into the use of meteoritic iron and into the

reconstruction of the evolution of metalworking technologies in the Mediterranean area.

Acknowledgements Natasha Almeida, Fabrizio Campanale, Aaron Cavosie, Massimo D’Orazio, Agnese Fazio, Gordon Osinski, Pierre Rochette, Sara Russell, and Romano Serra, made images available for this chapter. Massimo D’Orazio is thanked for helpful comments on an earlier version of the manuscript. LF’s research on Kamil Crater has been supported over the last decade by the Italian Ministero degli Affari Esteri e Cooperazione Internazionale—Progetti di Grande Rilevanza.

References

- Abate B, Koeberl C, Kruger FJ, Underwood JR Jr (1999) BP and Oasis impact structures, Libya, and their relation to Libyan Desert Glass. In: Dressler BO, Sharpton VL (eds) *Large meteorite impacts and planetary evolution II*, Geological Society of America Special Paper 339, pp 177–192
- Abu Aghreb AE, Ghadi AM, Schlüter J, Schultz L, Thiedig F (2003) Hamadah al Hamra and Dar al Gani: a comparison of two meteorite fields in the Libyan Sahara. In: 66th annual meteoritical society meeting (2003), abstract no. 5081
- Al-Kathiri A, Hofmann BA, Jull AJT, Gnos E (2005) Weathering of meteorites from Oman: correlation of chemical and mineralogical weathering proxies with ^{14}C terrestrial ages and the influence of soil chemistry. *Meteorit Planet Sci* 40:1215–1240
- Avicé G, Meier MMM, Marty B, Wieler R, Kramers JD, Langenhorst F, Cartigny P, Maden C, Zimmermann L, Andreoli MAG (2015) A comprehensive study of noble gases and nitrogen in “Hypatia”, a diamond-rich pebble from SW Egypt. *Earth Planet Sci Lett* 432:243–253
- Barakat AA (1991) Meteoritic iron from the Libyan glass area, southwestern Egypt. *Meteorit Planet Sci* 33:A173–A175
- Barakat AA (2012) The precious gift of meteorites and meteorite impact processes. Nova Sciences Publishers Inc, New York, p 166
- Barakat AA, De Michele V, Levi-Donati GR, Negro G, Serra R (1996) The desert of Great Sand Sea (GSS): an interesting reservoir of meteorite finds. *Meteorit Planet Sci* 31, A12 (abstract)
- Barakat AA, de Michele V, Negro G, Piacenza B, Serra R (1997) Some new data on the distribution of Libyan Desert Glass (Great Sand Sea, Egypt). In: de Michele V (ed) *Silica’96*, Proceedings of the meeting on Libyan Desert Glass and related Desert Events, Milan, Italy, Pyramids, pp 29–36
- Baratoux D, Chennaoui-Aoudjehane H, Gibson R, Lamali A, Reimold WU, Sapah SM, Chabou MC, Habarulema JB, Jessell MW, Mogessie A, Benkhaldoun Z, Nkhonjera E, Mukosi NC, Kaire M, Rochette P, Sickafoose A, Martínez-Frías J, Hofmann A, Folco L, Rossi AP, Faye G, Kolenberg K, Tekle K, Belhai D, Elyajouri M, Koeberl C, Abdeen MM (2017) The state of planetary and space sciences in Africa. *Eos* 98:16–23
- Baratoux D, Reimold WU (2016) The current state of knowledge about shatter cones: introduction to the special issue. *Meteorit Planet Sci* 51:1389–1434
- Barnes V, Underwood JR Jr (1976) New investigation of the strewn field of Libyan Desert Glass and its petrography. *Earth Planet Sci Lett* 30:117–122
- Barrat JA, Jahn BM, Amosse J, Rocchia R, Keller F, Poupeau GR, Diemer E (1997) Geochemistry and origin of Libyan Desert Glasses. *Geochim Cosmochim Acta* 61:1953–1959
- Bigazzi G, de Michele V (1997) New fission-track age determination on impact glasses. *Meteorit Planet Sci* 31:234–236
- Bland PA, Berry FJ, Smith TB, Skinner S, Pillinger CT (1996) Flux of meteorites to the Earth and weathering in hot desert ordinary chondrite finds. *Geochim Cosmochim Acta* 60:2053–2059
- Bland PA, Spurný P, Towner Martin C, Bevan AWR, Singleton AT, Bottke WF, Greenwood RC, Chesley SR, Shrubbený L, Borovička J, Ceplecha Z, McClafferty TP, Vaughan D, Benedix GK, Deacon G, Howard KT, Franchi IA, Hough RM (2009) An anomalous basaltic meteorite from the innermost main belt. *Science* 325:1525–1527
- Boslough MBE, Crawford DA (2008a) Low-altitude airbursts and the impact threat. *Int J Impact Eng* 35:1441–1448
- Boslough MBE, Crawford DA (2008b) Low-altitude airbursts and the impact threat. *Int J Impact Eng* 35:1441–1448
- Bridges JC, Warren PH (2006) The SNC meteorites: Basaltic igneous processes on Mars. *J Geol Soc London* 163:229–251
- Bridges JC, Catling DC, Saxton JM, Swindle TD, Lyon IC, Grady MM (2001) Alteration assemblages in martian meteorites: implications for near-surface processes. *Space Sci Rev* 96:365–392
- Cavosie AJ, Koeberl C (2019) Overestimation of threat from 100 Mt-class airbursts? High pressure evidence from zircon in Libyan Desert Glass. *Geology* 47:609–612
- Cavosie AJ, Timms NE, Erickson TM, Koeberl C (2018) New clues from Earth’s most elusive impact crater: evidence of reidite in Australasian tektites from Thailand. *Geology* 46:203–206
- Chambers (2006) Meteoritic diversity and planetesimal formation. In: Lauretta DS, McSween HY Jr (eds) *Meteorites and the early solar system II*, pp 487–497
- Chennaoui Aoudjehane H et al (2012) Tissint Martian meteorite: a fresh look at the interior, surface and atmosphere of Mars. *Science* 338 (6108):785–788
- Churcher CS, Mills AJ (1999) Reports from the Survey of Dakhleh Oasis, Western Desert of Egypt, 1977–1987. Oxbow Press, Oxford, p 271
- Churcher CS, Kleindienst MR, Schwarcz HP (1999) Faunal remains from a Middle Pleistocene lacustrine marl in Dakhleh Oasis, Egypt: palaeoenvironmental reconstructions. *Palaeogeogr Palaeoclimatol Palaeoecol* 154:301–312
- Clayton PA, Spencer LJ (1933) Lecture on the Libyan Desert Glass presented on the 9 November 1933 at the Annual Meeting of the Mineralogical Society. *Nature*, 501–508
- Cockell CS (2006) The origin and emergence of life under impact bombardment. *Philos Trans R Soc Lond B Biol Sci* 361(1474):1845–1856
- Collins GS, Melosh HJ, Osinski GS (2012) The impact-cratering process. *Elements* 8:25–30
- Comelli D, D’Orazio M, Folco L, El Halwagy M, Frizzi T, Alberti R, Capogrosso V, Elnaggar A, Hassan H, Nevin A, Porcelli F, Rashed MG, Valentini G (2016) The meteoritic origin of Tutankhamun’s iron dagger blade. *Meteorit Planet Sci* 51:1301–1309
- De Michele V (1998) The “Libyan Desert Glass” scarab in Tutankhamen’s pectoral. *Sahara* 10:107–109
- Deutsch A, Poelchau MH, Kenkmann T (2015) Impact metamorphism in terrestrial and experimental cratering events. In: Lee MR, Leroux H (eds) *Planetary mineralogy*. European Mineralogical Union, Notes in Mineralogy 15, Chapter 4, pp 89–127
- Diemer E (1997) Libyan Desert Glass: an impactite. State of the art in July 1996. In: de Michele V (ed) *Silica’96*, Proceedings of meeting on Libyan Desert Glass and related desert events, Milan, Italy, Pyramids, pp 29–36
- D’Orazio (2007) Meteorite records in the ancient Greek and Latin literature: between history and myth. In: Piccardi L, Masse WB (eds) *Myth and geology*. Geological Society London Special Publications 273, pp 215–225
- D’Orazio M, Folco L, Zeoli A, Cordier C (2011) Gebel Kamil: the iron meteorite that formed the Kamil Crater (Egypt). *Meteorit Planet Sci* 46:1179–1196

- El-Baz F (1981) Circular feature among dunes of the Great Sand Sea, Egypt. *Science* 213:439–440
- El-Baz F, Ghoneim E (2007) Largest crater shape in the Great Sahara revealed by multi-spectral images and radar data. *Int J Remote Sens* 28(2):451–458
- Erickson TM, Cavosie AJ, Moser DE, Barker IR, Radovan HA, Wooden J (2013) Identification and provenance determination of distally transported, Vredefort-derived shocked minerals in the Vaal River, South Africa using SEM and SHRIMP-RG techniques. *Geochim Cosmochim Acta* 107:170–188
- Fazio A, Folco L, D’Orazio M, Frezzotti ML, Cordier C (2014) Shock metamorphism and impact melting in small impact craters on Earth: evidence from Kamil Crater, Egypt. *Meteoritics and Planetary Science* 49:2175–2200
- Fazio A, D’Orazio M, Cordier C, Folco L (2016) Target-projectile interaction during impact melting at Kamil Crater, Egypt. *Geochimica et Cosmochimica Acta* 18:33–50
- Ferrière L, Osinski G (2013) Shock metamorphism. In: Osinski GR, Pierazzo E (eds) *Impact cratering—processes and products*. Wiley-Blackwell, Oxford
- Folco L, Di Martino M, El Barkooky A, D’Orazio M, Lethy A, Urbini S, Nicolosi I, Hafez M, Cordier C, van Ginneken M, Zeoli A, Radwan AM, El Khrepy S, El Gabry M, Gomaa M, Barakat AA, Serra R, El Sharkawi M (2010) The Kamil Crater in Egypt. *Science* 329:804
- Folco L, Di Martino M, El Barkooky A, D’Orazio M, Lethy A, Urbini S, Nicolosi I, Hafez M, Cordier C, van Ginneken M, Zeoli A, Radwan AM, El Khrepy S, El Gabry M, Gomaa M, Barakat AA, Serra R, El Sharkawi M (2011) Kamil Crater (Egypt): ground truth for small scale meteorite impact on earth. *Geology* 39:179–182
- Folco L, D’Orazio M, Fazio A, Cordier C, Zeoli A, van Ginneken M, Barkooky A (2015) Microscopic impactor debris in the soil around Kamil Crater (Egypt): inventory, distribution, total mass and implications for the impact scenario. *Meteorit Planet Sci* 50:382–400
- French BM, Koeberl C (2010) The convincing identification of terrestrial meteorite impact structures: What works, what doesn’t, and why? *Earth Sci Rev* 98:123–170
- Fröhlich F, Poupeau G, Badou A, Le Bourdonnec FX, Sacquin Y, Dubernet JM, Bardintzeff M, Vêran M, Smith DC, Diemer E (2013) Libyan Desert Glass: new field and Fourier transform infrared data. *Meteorit Planet Sci* 48, 2517–2530
- Fudali RF (1981) The major element chemistry of Libyan Desert Glass and the mineralogy of its precursor. *Meteoritics* 16:247–259
- Gattacceca J, Valenzuela M, Uehara M, Jull AJ, Giscard M, Rochette P, Braucher R, Suavet C, Gounelle M, Morata D, Munayco P, Bourrot-Denise M, Bourles D, Demory F (2011) The densest meteorite collection area in hot deserts: the San Juan meteorite field (Atacama Desert, Chile). *Meteorit Planet Sci* 46:1276–1287
- Gibson RL, Reimold WU (2008) *The geology of the Vredefort impact structure. Memoir 97, Council for Geoscience, Pretoria, South Africa*, 181 pp
- Gillet P, El Goresy A (2013) Shock events in the solar system: the message from minerals in terrestrial planets and asteroids. *Ann Rev Earth Planet Sci* 41, 12.1–12.29
- Giuli G, Paris E, Pratesi G, Koeberl C, Cipriani C (2003) Iron oxidation state in Fe-rich layer and silica matrix of Libyan Desert Glass: a high-resolution XANES study. *Meteorit Planet Sci* 38:1181–1186
- Glass BP, Simonson BM (2012) Distal impact ejecta layers: Spherules and more. *Elements* 8:43–48
- Goderis S, Paquay F, Claeys P (2013) Projectile identification in terrestrial impact structures and ejecta material. In: Osinski GR, Pierazzo E (eds) *Impact cratering—processes and products*. Wiley-Blackwell, Oxford, pp 1–20
- Greshake A, Koeberl C, Fritz J, Reimold WU (2010) Brownish inclusions and dark streaks in Libyan Desert Glass: evidence for high-temperature melting of the target rock. *Meteorit Planet Sci* 45:973–989
- Greshake A, Wirth R, Fritz J, Jakubowsky T, Böttger U (2018) Mullite in Libyan Desert Glass: evidence for high-temperature/low-pressure formation. *Meteorit Planet Sci* 53:467–481
- Halliday I, Blackwell AT, Griffin AA (1978) The Innisfree meteorite and the Canadian camera network. *J R Astron Soc Canada* 72:15–39
- Hamann C, Fazio A, Ebert M, Hecht L, Folco L, Deutsch A, Wirth R, Reimold WU (2018) Silicate liquid immiscibility in impact melts. *Meteorit Planet Sci* (in press) 53:1594–1632
- Hargitai H, Reimold WU, Bray VJ (2015) Impact structure. In: Hargitai H, Kereszturi Á (eds) *Encyclopedia of planetary landforms*, vol. 2. Springer Science + Business Media LLC, New York, pp 988–1023
- Horn P, Müller-Sohnius D, Schaaf P, Kleinmann B, Storzer D (1997) Potassium-argon and fission-track dating of Libyan Desert Glass, and strontium- and neodymium isotope constraints on its source rock. In: de Michele V (ed) *Proceedings of the silica ’96 meeting on Libyan Desert Glass and related desert events*, Bologna, Segrate, Italy: Pyramids, pp 59–73
- Hutzler A, Gattacceca J, Rochette P, Braucher R, Carro B, Christensen EJ, Courmede C, Gounelle M, Laridhi Ouazaa N, Martinez R, Valenzuela M, Warner M, Bourles D (2016) Description of a very dense meteorite collection area in western Atacama: insight into the long-term composition of the meteorite flux to Earth. *Meteorit Planet Sci* 51:468–482
- Issawi B (1982) Geology of the southwestern desert of Egypt. In: El-Baz F, Maxwell TA (eds) *Desert landforms of Southwest Egypt: a basis for comparison with Mars*. National Air and Space Museum, Washington, DC, pp 57–66
- Johnson D, Tyldesley J, Lowe T, Withers PJ, Grady MM (2013) Analysis of a prehistoric Egyptian iron bead with implications for the use and perception of meteorite iron in ancient Egypt. *Meteorit Planet Sci* 48:997–1006
- Jull AJT (2006) Terrestrial ages of meteorites. In: Lauretta DS, McSween HY Jr (eds) *Meteorites and the early solar system II*, pp 889–905
- Kenkmann T, Deutsch A, Thoma K, Poelchau M (2013) The MEMIN experimental impact cratering. *Meteorit Planet Sci* 48(1):164 (Special Issue)
- Klein J, Giegengack R, Middleton R, Sharma P, Underwood JR Jr, Weeks RA (1986) Revealing histories of exposure using in situ produced ^{26}Al and ^{10}Be in Libyan Desert Glass. *Radiocarbon* 28:547–555
- Kleinmann B (1969) The breakdown of zircon observed in the Libyan Desert Glass as evidence of its impact origin. *Earth Planet Sci Lett* 5:497–501
- Kleinmann B, Horn P, Langenhorst F (2001) Evidence for shock metamorphism in sandstones from the Libyan Desert Glass strewn field. *Meteorit Planet Sci* 36:1277–1282
- Klitzsch E, List FK, Pöhlmann G (1987) *Geologic map of Egypt 1:500000*. The Egyptian General Petroleum Corporation, Cairo, Egypt, 20 sheets
- Koeberl C (1997) Libyan Desert Glass: geochemical composition and origin. In: de Michele V (ed) *Proceedings of the Silica ’96 meeting on Libyan Desert Glass and related desert events*, Bologna, Pyramids, Segrate, Milano, pp 121–131
- Koeberl C (2000) Confirmation of a meteoritic component in Libyan Desert Glass from osmium isotopic data. *Meteorit Planet Science* 35. A89–A90 (abstract)
- Koeberl C (2014) The geochemistry and cosmochemistry of impacts. In: Holland HD, Turekian KK (eds) *Treatise on geochemistry*, vol 2, 2nd edn. Elsevier, Oxford, pp 73–118
- Koeberl C, Claeys Ph, Hecht L, McDonald I (2012) Geochemistry of impactites. *Elements* 8:37–42

- Koerberl C, Ferrière L (2019) Libyan Desert Glass area in western Egypt: shocked quartz in bedrock points to a possible deeply eroded impact structure in the region. *Meteorit Planet Sci* (in press). <https://doi.org/10.1111/maps.13250>
- Kramers JD, Andreoli MAG, Atanasova M, Belyanin GA, Block D, Franklyn C, Harris C, Lekgoathi M, Montross CS, Ntsoane T, Pischedda V, Segonyane P, Viljoen KS, Westraadt JE (2013) Unique chemistry of a diamond-bearing pebble from the Libyan Desert Glass strewnfield, SW Egypt: evidence for a shocked comet fragment. *Earth Planet Sci Lett* 382:21–31
- Krot AN, Keil K, Scott ERD, Goodrich CA, Weisberg MK (2014) Classification of meteorites and their genetic relationships. In: Davis AM (ed) *Meteorites and cosmochemical processes*, volume 1 of treatise on geochemistry, 2nd edn, pp 1–63
- Langerhorst F, Deutsch A (2012) Shock metamorphism of minerals. *Elements* 8:31–36
- Longinelli A, Sighinolfi G, De Michele V, Selmo E (2011) $\delta^{18}\text{O}$ and chemical composition of Libyan Desert Glass, country rocks, and sands: new considerations on target material. *Meteorit Planet Sci* 46:218–227
- Magna T, Deutsch A, Mezger K, Skála R, Seitz H-M, Mizera J, Řanda Z, Adolph L (2011) Lithium in tektites and impact glasses: implications for sources, histories and large impacts. *Geochimica et Cosmochimica Acta* 75, 2137–2158
- Martin AJ (1969) Possible impact structure in Southern Cyrenaica, Libya. *Nature* 223:940–941
- Matsubara K, Matsuda J, Koerberl C (1991) Noble gases and K–Ar ages in Auelloul, Zhamanshin, and Libyan Desert impact glasses. *Geochim Cosmochim Acta* 55:2951–2955
- McCoy TJ, Mittlefehldt DW, Wilson L (2006) Asteroid differentiation. In: Lauretta DS, McSween HY Jr (eds) *Meteorites and the early solar system II*, pp 733–745
- McCrosky RE, Posen A, Schwartz G, Shao C-Y (1971) Lost City meteorite—its recovery and a comparison with other fireballs. *J Geophys Res* 76:4090–4108
- McSween HY, McLennan SM (2014) Mars. In: Davis AM (ed) *Planets, asteroids, comets and the solar system*, volume 2 of treatise on geochemistry, 2nd edn. Elsevier, pp. 251–300
- McSween HY, Lauretta DS, Lexhin LA (2006) Recent advances in meteoritics and cosmochemistry. In: Lauretta DS, McSween HY Jr (eds) *Meteorites and the early solar system II*, pp. 53–66
- Melosh HJ (1989) *Impact cratering: a geologic process*. Oxford monographs on geology and geophysics. Oxford University Press, Oxford, p 245
- Murali AV, Linstrom EJ, Zolensky ME, Underwood JR Jr, Giegengack RF (1989) Evidence of extraterrestrial components in the Libyan Desert Glass (abstract). *EOS Trans AGU* 70:1178
- Murali AV, Zolensky ME, Underwood JR Jr, Giegengack RF (1997) Chondritic debris in Libyan Desert Glass. In: de Michele V (ed.) *Proceedings of Silica'96 meeting on Libyan Desert Glass and related desert events*, Milan, Italy, Pyramids, pp 133–142
- Negro G, Damiano-Appia M (1992) Il “Silica Park”: un centro di lavorazione del LDSG nel Great Sand Sea. *Sahara* 5:105–108
- Oakley KP (1952) Dating the Libyan Desert Silica Glass. *Nature* 170:447–449
- Oberst J, Molau S, Heinlein D, Gritznier C, Schindler M, Spurny P, Cepelcha Z, Rendtel J, Betlem H (1998) The “European Fireball Network”: current status and future prospects. *Meteorit Planet Sci* 33:49–56
- Orti L, Di Martino M, Morelli M, Cigolini C, Pandeli E, Buzzigoli A (2008) Nonimpact origin of the crater-like structures in the Gilf Kebir area (Egypt): implications for the geology of eastern Sahara. *Meteorit Planet Sci* 43:1629–1639
- Osinski GR (2008) Meteorite impact structures: the good and the bad. *Geol Today* 24:13–19
- Osinski GR, Schwarcz HP, Smith JR, Kleindienst MR, Haldemann AFC, Churcher CS (2007) Evidence for a ~200–100 ka meteorite impact in the Western Desert of Egypt. *Earth Planet Sci Lett* 253:378–388
- Osinski GR, Kieniewicz J, Smith JR, Boslough MBE, Eccleston M, Schwarcz HP, Kleindienst MR, Haldemann AFC, Churcher CS (2008) The Dakhleh Glass: product of an airburst or cratering event in the Western Desert of Egypt? *Meteorit Planet Sci* 43:2089–2107
- Ott U, Merchel S, Herrman T, Pavetich S, Rugel G, Faestermann T, Fimiani L, Gomez-Guzman JM, Hain K, Korschinek G, Ludwig P, D’Orazio M, Folco L (2014) Cosmic ray exposure and pre-atmospheric size of the Gebel Kamil iron meteorite. *Meteorit Planet Sci* 49:1365–1374
- Paillou P, El-Barkooky A, Barakat A, Melezieux JM, Reynard B, Dejax J, Heggy E (2004) Discovery of the largest impact crater field on Earth in the Gilf Kebir region, Egypt. *Compte Rendus Géoscience de l’Académie de Sciences* 336:1491–1500
- Paillou P, Reynard B, Malezieux JM, Dejax J, Heggy E, Rochette P, Reimold WU, Michel P, Baratoux D, Razin P, Colin JP (2006) An extended field of crater-shaped structures in the Gilf Kebir region, Egypt: observations and hypotheses about their origin. *J Afr Earth Sci* 46:281–299
- Pierazzo E, Artemieva NA (2012) Local and global environmental effects of impacts on Earth. *Elements* 8:55–60
- Pratesi G, Viti C, Cipriani C, Mellini M (2002) Silicate-Silicate liquid immiscibility and graphite ribbons in Libyan Desert Glass. *Geochim Cosmochim Acta* 66:903–911
- Rehren T, Belgya T, Jambon A, Káli G, Kasztovszky Z, Kis Z, Kovács I, Maróti B, Martín-Torres M, Miniaci G, Pigott VC, Radivojević M, Rosta L, Szentmiklósi L, Szokefalvi-Nagy Z (2013) 5,000 years old Egyptian iron beads made from hammered meteoritic iron. *J Archaeol Sci* 40:4785–4792
- Reimold U, Jourdan F (2012) Impact!—Bolides, craters and catastrophes. *Elements* 8:19–24
- Reimold U, Koerberl C (2014) Impact structures in Africa: a review. *J Afr Earth Sci* 93:57–175
- Reimold WU, Koerberl C, Gibson RL, Dressler BO (2005) Economic mineral deposits in impact structures: a review. In: Koerberl C, Henkel H (eds) *Impact tectonics, impact studies series*, vol 6, Springer, pp 479–552
- Renne PR, Schwarcz HP, Kleindienst MR, Osinski GR, Donovan JJ (2010) Age of the Dakhleh impact event and implications for Middle Stone Age archeology in the Western Desert of Egypt. *Earth Planet Sci Lett* 291:201–206
- Rocchia R, Robin E, Fröhlich F, Amosse J, Barrat J-A, Méon H, Froget L, Diemer E (1997) The impact origin of Libyan Desert Glass. In: de Michele V (ed) *Proceedings of Silica’96 meeting on Libyan Desert Glass and related desert events*, Milan, Italy, Pyramids, pp 143–149
- Roe DA, Olsen JW, Underwood Jr, Giegengack RF (1982) A handaxe of Libyan Desert Glass. *Antiquity* LVI, 88–92
- Roperch P, Gattacceca J, Valenzuela M, Devouard B, Lorand J-P, Arriagada C, Rochette P, Latorre C, Beck P (2017) Surface vitrification caused by natural fires in Late Pleistocene wetlands of the Atacama Desert. *Earth Planet Sci Lett* 469:15–26
- Rubin AE, Grossman JN (2010) Meteorite and meteoroid: new comprehensive definitions. *Meteorit Planet Sci* 45:114–122
- Russell SS, Hartman L, Cuzzi J, Krot AN, Gounelle M, Weidenschilling S (2006) Timescales of the solar protoplanetary disk. In: Lauretta DS, McSween HY Jr (eds) *Meteorites and the early solar system II*, pp 233–251
- Schaaf P, Müller-Sohnius D (2002) Strontium and neodymium isotopic study of Libyan Desert Glass: inherited Pan-African age signatures and new evidence for target material. *Meteorit Planet Sci* 37:565–576

- Schlüter J, Schultz L, Thiedig F, Al-Mahdi BO, Abu Aghreb AE (2002) The Dar al Gani meteorite field (Libyan Sahara): geological setting, pairing of meteorites, and recovery density. *Meteorit Planet Sci* 37, 1079–1093
- Scott ERD, Krot AN (2014) Chondrites and their components. In: Davis AM (ed) *Meteorites and cosmochemical processes*, volume 1 of *Treatise on geochemistry*, 2nd edn, pp 65–137
- Sighinolfi GP, Sibilia E, Contini G, Martini M (2015) Thermoluminescence dating of the Kamil impact crater (Egypt). *Meteorit Planet Sci* 50:204–213
- Stöffler D, Grieve RAF (2007) Impactites. In: Fettes D, Desmons J (eds) *Metamorphic rocks: a classification and glossary of terms, recommendations of the international union of geological sciences*. Cambridge University Press, Cambridge, UK, pp 82–92, 111–125, and 126–242 (Chapter 2.11)
- Stöffler D, Hamann C, Metzler K (2018) Shock metamorphism of planetary silicate rocks and sediments: proposal for an updated classification system. *Meteorit Planet Sci* 53:5–49
- Storzer D, Koeberl C (1991) Uranium and zirconium enrichments in Libyan Desert Glass. Zircon, baddeleyite and high temperature history of the glass. *Lunar Planet Sci XXII*, 1345–1346
- Storzer D, Wagner GA (1977) Fission-track dating of meteorite impacts. *Meteoritics* 12:368–369
- Swaenen M, Stefaniak EA, Frost R, Worobiec A, Grieken RV (2010) Investigation of inclusions trapped inside Libyan Desert Glass by Raman microscopy. *Analyt Bioanalyt Chem* 397:2659–2665
- Treiman AH (2005) The nakhlite meteorites: Augite-rich igneous rocks from Mars. *Chemie Erde* 65:203–270
- Underwood JR Jr, Fisk EP (1980) Meteorite impact structures, Southeast Libya. In: Salem MJ, Busrewil MT (eds) *The geology of Libya 3, 2*. Symposium on the Geology of Libya 1978, London, pp 893–900
- Urbini S, Nicolosi I, Zeoli A, El Khrepy S, Lethy A, Hafez M, El Gabry M, El Barkooky A, Barakat A, Gomaa M, Radwan A, El Sharkawi M, D’Orazio M, Folco L (2012) Geological and geophysical investigation of Kamil Crater, Egypt. *Meteorit Planet Sci* 47:1842–1868
- Warren PH, Taylor GJ (2014) The moon. In: Davis AM (ed) *Planets, asteroids, comets and the solar system*, Volume 2 of *Treatise on geochemistry*, 2nd edn. Elsevier, pp 213–250
- Wasson JT (2003) Large aerial bursts: an important class of terrestrial accretionary events. *Astrobiology* 3:163–179
- Weeks RA, Underwood JR Jr, Giegengack R (1984) Libyan Desert glass: a review. *J Non-Cryst Solids* 67, 593–619